

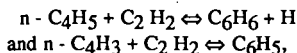
THE FORMATION OF BENZENE IN FLAMES

James A. Miller and Carl F. Melius
Sandia National Laboratories
Livermore, CA 94551-0969

Introduction

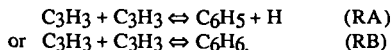
The mechanism by which aromatic compounds are formed in flames of aliphatic fuels is currently a "hot topic" in combustion. This interest stems from the importance of small aromatic compounds in the formation of PAH (polycyclic aromatic hydrocarbons) and soot (undesirable by-products) in combustion processes. The formation of the "first ring" is a key step in such processes and may well be rate limiting. The identification of the elementary reactions leading to the first aromatic compound consequently is of paramount importance.

Perhaps the two most cited reactions leading to cyclization (i.e., ring formation) are the reactions,



where C_6H_6 is benzene and C_6H_5 is phenyl. Unfortunately, both $n-C_4H_3$ and $n-C_4H_5$ have isomers, $i-C_4H_3$ and $i-C_4H_5$, that are more stable than they are, and distinguishing between the isomers on a mass spectrometer (the diagnostic tool in most flame experiments) is impossible. Consequently, to determine the extent to which these reactions occur in a flame requires a thorough understanding of the "pre-cyclization" chemistry. In fact, a thorough understanding of the pre-cyclization chemistry is essential in determining what the cyclization steps are in any event.

In the present paper, we review the mechanism we have proposed previously^(1,2) for the formation of C_3 and C_4 hydrocarbons in rich acetylene flames. In doing this we compare the predictions of our kinetic model with the experimental results of Bastin, et al.⁽³⁾ and Westmoreland,⁽⁴⁾ in lightly sooting $C_2H_2/O_2/Ar$ flames. In addition, we discuss the implausibility of reactions (R191) and (R190) (reaction numbers refer to the table in Ref. 1) as primary cyclization steps in such flames. We show that the reaction between two propargyl radicals,



is a much better candidate for forming the first ring. This leads us to perform extensive BAC-MP4 calculations on this reaction and to interpret the extensive amount of low-temperature pyrolysis data on non-aromatic C_6H_6 compounds in terms of this potential.

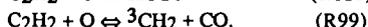
FLAME CALCULATIONS, CHEMICAL KINETICS, AND THERMODYNAMICS

The flame calculations discussed in this paper were performed in the same manner as described previously,^(1,2) using the Sandia flame code.^(5,6) Thermodynamic data come primarily from the Chemkin thermodynamic data base,⁽⁷⁾ supplemented by BAC-MP4 results for some key

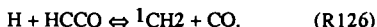
C₃ and C₄ species. These species have subsequently been added to the Chemkin data base. The reaction mechanism is the same as that described in Refs. 1 and 2. This mechanism utilizes the rate coefficient expressions given by Westmoreland for reactions (R190) and (R191).

THE FORMATION OF C₃ AND C₄ HYDROCARBONS

Even in sooting acetylene flames the dominant C₂H₂ removal step is the two - channel reaction,



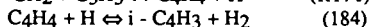
In rich flames, the ketyl formed in reaction (R100) reacts primarily with hydrogen atoms to form ¹CH₂,



The presence of ¹CH₂ in these flames has important consequences for the formation mechanism of C₃ and C₄ hydrocarbons.

Singlet methylene, ¹CH₂, inserts rapidly into acetylene, forming propargyl and a hydrogen atom,
$${}^1\text{CH}_2 + \text{C}_2\text{H}_2 \rightleftharpoons \text{C}_3\text{H}_3 + \text{H}. \quad (\text{R143})$$

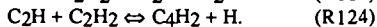
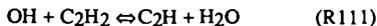
Reaction (R143) is the primary source of propargyl, which is principally consumed by reaction with H-atoms. Vinyl acetylene (C₄H₄) and C₄H₃ are formed by the reactions.



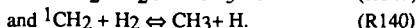
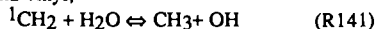
Diacetylene, C₄H₂, comes from



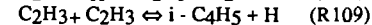
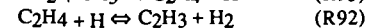
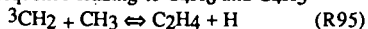
as well as the sequence



Butadiene and the butadienyl radical, C₄H₆ and C₄H₅, are formed from ¹CH₂ by circuitous routes through ethylene and vinyl,



Reactions (R140) and (R141) are the most important sources of methyl in these flames. There then follows the reaction sequence leading to C₄H₆ and C₄H₅



Figures 1 and 2 show comparisons of our model predictions with the experiments of Westmoreland for C₃H₃ and with those of Bastin et al. for C₄H₃ and C₄H₅. Many other comparisons are shown in Refs. 1 and 2.

FORMATION OF BENZENE

In the reaction mechanism of Ref. 1, there are only two ways to form benzene,



followed by phenyl either adding or abstracting a hydrogen atom, and

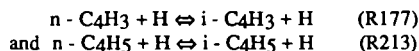


Because of the low levels of both isomers of C₄H₅ in the flame, neither (R190) nor its *i*-C₄H₅ counterpart is ever an effective route to benzene formation in our model. Consequently, all the benzene formed is through phenyl. In competition for phenyl with reactions that produce benzene are the oxidative paths.



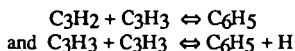
In order to be conservative about eliminating reactions as possible sources for benzene, we have in some cases added the C₆H₆ and C₆H₅O predictions to compare with the experimental benzene profiles

Figure 3 shows comparisons of model predictions with the experimental results for benzene from Bastin, et al.⁽³⁾. The basic model is unable to predict the benzene concentrations measured in the flame primarily because of the reactions,



which render the *n*-isomers very small fractions the total radical concentrations in the flame. Even increasing *k*₁₉₈ and *k*₁₉₇ by a factor of ten (an unreasonable increase) does not result in sufficient benzene levels. Neither does including reactions of *i*-C₄H₃ and *i*-C₄H₅ with acetylene to form benzene. The fact that case (d) in Fig. 3 comes close to the experiment really implies that all the C₄H₃ would have to be the *i*-isomer to predict the benzene levels observed.

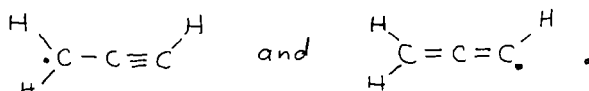
From Fig. 3 one can see that only the reactions,



are capable of predicting the benzene levels observed in the flame. The first of these reactions, because of the high rate coefficient required and because our model overpredicts the C₃H₂ concentrations observed by Westmoreland (thus implying an even higher rate coefficient), is a less attractive candidate than the second. The second reaction, the recombination of two propargyl radicals, has been suggested as a source of benzene in shock tube experiments on the pyrolysis of allene and propyne by Kern and co-workers^(8,9) and, independently and concurrently with our work, ⁽¹⁾ has been suggested by Stein, et al. ⁽¹⁰⁾ as a possible source of benzene in acetylene flames.

PROPARGYL RADICAL RECOMBINATION

In order to test the viability of forming an aromatic compound, i.e., either $C_6H_5 + H$ or C_6H_6 , from the recombination of two propargyl radicals, we have performed an extensive set of BAC-MP4 electronic structure calculations. The results are presented in Figs. 4 and 5. Propargyl is a resonantly stabilized radical with the two structures,



If we refer to the end of the radical with two hydrogens as the head and the end with one hydrogen as the tail, Fig. 4 shows the intermediate structures and potential energy barriers encountered in head-to-head or tail-to-tail recombination, and Fig. 5 shows those encountered in head-to-tail recombination.

Our potential is at least qualitatively consistent with a variety of low-temperature pyrolysis experiments⁽¹⁰⁾ which show 3,4-dimethylenecyclobutene  and fulvene  as primary products of both 1,5-hexadiyne ($\equiv - - - \equiv$) pyrolysis and 1,2,4,5-hexatetraene ($= - - =$) pyrolysis. Our one inconsistency with these experiments is the implication that there is a low energy path to benzene from 1,5-hexadiyne and 1,2,4,5-hexatetraene. We have not yet found one. The implication of these results we discussed in Ref. 1. However, we do find an energetically accessible path from $C_3H_3 + C_3H_3$ to benzene and to phenyl + H via head-to-tail recombination, as shown in Fig. 5. Thus, our calculations confirm the possibility of forming benzene in flames by a relatively fast reaction between two propargyl radicals. Such a result is also consistent with the experiments of Alkemade and Homann⁽¹¹⁾, which show a fast $C_3H_3 + C_3H_3$ rate coefficient and show benzene as a major product.

Acknowledgement: This work is sponsored by the U.S. Department of Energy, Office of Basic Energy Sciences, Division of Chemical Sciences

References

1. Miller, J. A. and Melius, C. F. : "Kinetic and Thermodynamic Issues in the Formation of Aromatic Compounds in Flames of Aliphatic Fuels," *Combustion and Flame* (submitted)
2. Miller, J. A., Volponi, J. V., Durant, J. L., Goldsmith, J. E. M., and Kee, R. J.: "The Structure and Reaction Mechanism of Rich Non-Sooting $C_2H_2/O_2/Ar$ Flames", *Twenty-Third Symposium (International) on Combustion*, in press (1991)
3. Bastin, E., Delfau, J-L, Reuillon, M., Vovelle, C., and Warnatz, J.: *Twenty Second Symposium (International) on Combustion*, p. 313, The Combustion Institute (1989)
4. Westmoreland, P.R., Thesis Chem. Eng. Dept., M. I. T. 1986
Westmoreland, P. R., Dean, A. M., Howard, J. B. and Longwell, J. P. : *J. Phys. Chem.* 93, 8171 (1989)
5. Kee, R. J., Grcar, J. F., Smooke, M. D., and Miller, J. A.: "A Fortran Program for Modeling Steady, Laminar, One-Dimensional, Premixed Flames," Sandia Technical Report SANDS85-8240, Sandia National Laboratories, Livermore, CA, December 1985
6. Grcar, J. F., Kee, R. J., Smooke, M. D., and Miller, J. A.: *Twenty-First Symposium (International) on Combustion*, p. 1773, The Combustion Institute (1987)
7. Kee, R. J., Rupley, F. M., and Miller, J. A.: "The Chemkin Thermodynamic Data Base", Sandia Technical Report SAND87-8215, Sandia National Laboratories, Livermore, CA, April 1987
8. Wu, C. H. and Kern, R. D.: *J. Phys. Chem.* 91, 6291, (1987)
9. Kern, R. D., Singh, H. J. and Wu, C. H.: *Int. J. Chem. Kin.* 20, 731 (1988)
10. Stein, S. E., Walker, J. R., Suryan, M. M., and Fahr, A.: "A New Path to Benzene in Flames," *Twenty-Third Symposium (International) on Combustion*, in press (1991) and references cited therein
11. Alkemade, U. and Homann, K. H.: *J. Phys. Chem. Neue Folge* 161, 19-34 (1989)

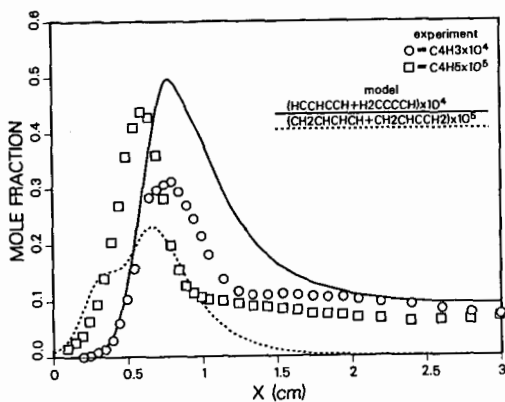


Figure 1. Comparison of model predictions with the experiments of Bastin, et al. for C_4H_3 and C_4H_5 .

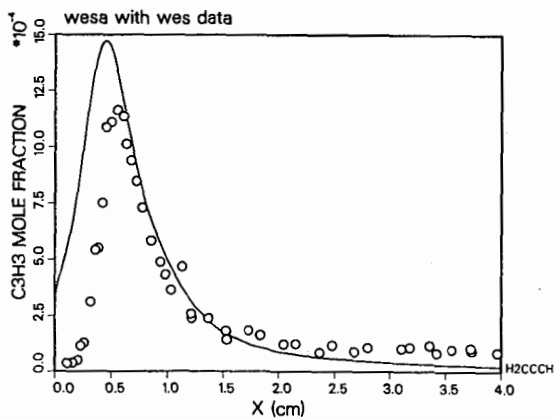


Figure 2. Comparison of model predictions with the experiments of Westmoreland for C_3H_3 .

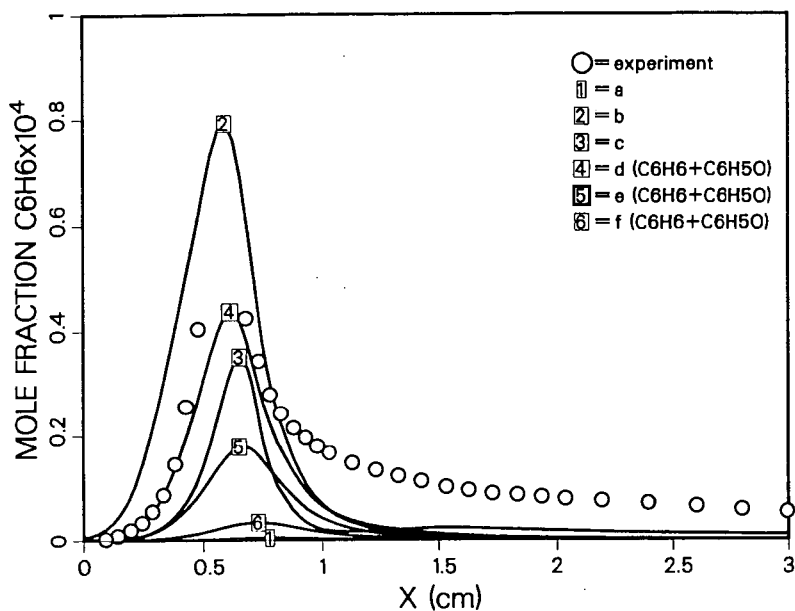


Figure 3 Comparison of model predictions with the experiments of Bastin, et al. for benzene (a) model of Ref. 1, (b) model of Ref. 1 with the addition of $C_3H_3 + C_3H_3 \rightleftharpoons C_6H_5 + H$ ($k = 1 \times 10^{13} \text{cm}^3/\text{mole sec}$); (c) model of Ref. 1 with the addition of $C_3H_3 + C_3H_2 \rightleftharpoons C_6H_5$ ($k = 5 \times 10^{13} \text{cm}^3/\text{mole-sec.}$); (d) model of Ref. 1 with the addition of $i-C_4H_3 + C_2H_2 \rightleftharpoons C_6H_5$ and $i-C_4H_5 + C_2H_2 \rightleftharpoons C_6H_6 + H$ (same rate coefficients as for the analogous $n-C_4H_3$ and $n-C_4H_5$ reactions); (e) model of Ref. 1 with k_{190} and k_{191} increased by a factor of ten; (f) model of Ref. 1 with the heat of formation of $i-C_4H_3$ increased to 121.7 kcal/mole. In cases d, e, and f, the predictions are for the sum of C_6H_6 and C_6H_5O

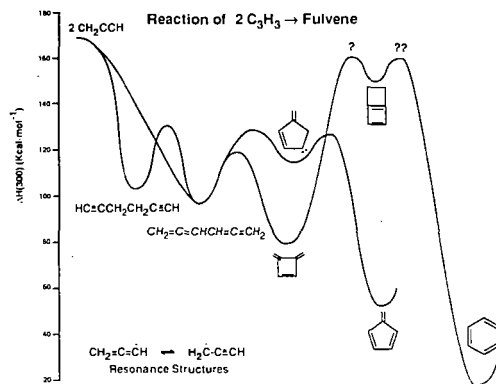


Figure 4. Potential energy diagram for head-to-head or tail-to-tail recombination of two propargyl radicals.

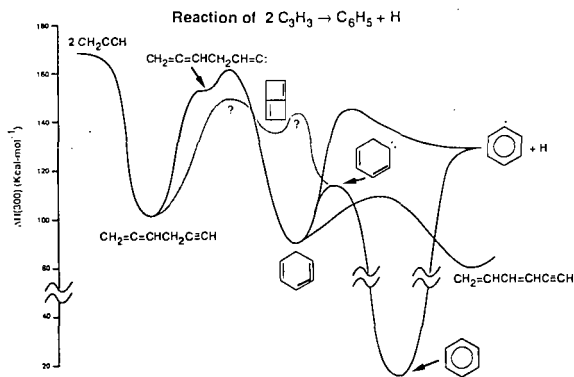


Figure 5. Potential energy diagram for head-to-tail recombination of two propargyl radicals.

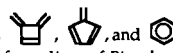
C₃H₃ REACTION KINETICS IN FUEL-RICH COMBUSTION

S. D. Thomas, F. Communal, P. R. Westmoreland
Department of Chemical Engineering, University of Massachusetts
Amherst, MA 01003

Keywords: propargyl, chemical activation, benzene

ABSTRACT

At typical flame temperatures and pressures, we predict that direct propargyl (C₃H₃) combination forms the open-chain C₆H₆ species 1,5-hexadiyne, 1,2,4,5-hexatetraene, and 4,5-hexadienyne in preference to cyclic C₆H₆ species 3,4-dimethylenecyclobutene, fulvene, and

benzene () vs. ). These chemically activated reactions, analyzed by a new Q-formalism of Bimolecular Quantum-RRK, have rate constants and rates that are consistent with C₆H₆ data from a C₂H₂/O₂/Ar flat flame. Cyclic C₆H₆'s may then be generated by thermal isomerizations.

INTRODUCTION

Recently, C₃H₃ has been the subject of intense interest as a possible precursor to aromatics in flames.¹⁻⁸ In earlier work, Hurd and co-workers proposed in 1962 that aromatics might be formed by combination of trimethine (CHCHCH)⁹, and Tsang had encouraged others to explore propargyl (·CH₂-C≡CH or CH₂=C=CH·) as an aromatics precursor based on his high soot yields from pyrolysis experiments.¹⁰ Kern and co-workers provided the first experimental evidence and mechanism for C₆H₆ formation from C₃H₃,^{1,2} stimulating much of the subsequent research.

In 1989 we proposed⁴ a chemically activated pathway from C₃H₃ to benzene (Figure 1), similar to that of Kern, and presented preliminary calculations of its feasibility. The electron density of propargyl is best represented as propynyl¹³ although it is a resonance structure of propynyl and propadienyl (CH=C-CH₂· and ·CH₂=C=CH₂). Propynyls may combine to make chemically activated 1,5-hexadiyne ("hot" 1,5-hexadiyne). The hot adduct may isomerize by a Cope rearrangement to hot 1,2,4,5-hexatetraene, which may isomerize to make hot 3,4-dimethylenecyclobutene (DMCB) by a sigmatropic ring closure analogous to that of 1,3-butadiene forming cyclobutene. DMCB can isomerize to hot fulvene (methylenecyclopentadiene) which can isomerize to hot benzene. Because of chemical activation, the energy released into the first adduct by bond formation, each of these steps occurs above the intrinsic or thermal energy barriers. Each one of these chemically activated isomers may be stabilized by bimolecular collisions, or it may decompose or isomerize unimolecularly. This hypothesized route was based on thermal pyrolyses of 1,5-hexadiyne to DMCB, fulvene, and benzene;¹¹⁻¹⁵ pyrolysis of hexatetraene to the same products;¹⁴ pyrolysis of DMCB to fulvene and benzene;¹⁵ and pyrolysis of fulvene to benzene.^{15,16} Compared to the route of Kern and coworkers,² this route could proceed without thermal intermediates and without diradicals.

Independently and at the same time, and Stein developed a route similar to that in Figure 1,⁵ and Alkemade and Homann proposed a fourth, quite different route.³ Stein pyrolyzed 1,2-hexadiyne at different temperatures in a VLPP reactor. At low temperatures, DMCB was formed, while at higher temperatures, fulvene and benzene were formed apparently from a DMCB intermediate; Stein proposed that parallel paths to the two products may occur. Alkemade and Homann have made the only direct experimental studies of C₃H₃ combination, finding a mixture of products including benzene. Their mechanism involved cyclopropenyl intermediates similar to those proposed as intermediates in propyne/propadiene isomerization.¹⁷

More recently, Miller and Melius⁷ have proposed a fifth route via 4,5-hexadienyne, the head-to-tail combination product of propargyls. They suggest rearrangement of the acetylenic group to a vinylidene form, which would insert into an allenic C-H bond to form a 1,2,4-cyclohexatriene. Finally they suggest rapid rearrangement to benzene, apparently by a molecular 1,3 H-shift.

Most of these routes are energetically feasible, but there are energetic and entropic challenges to overcome en route. Direct closure to a six-membered ring requires a tight transition state with loss of internal rotation(s), and 1,2- or 1,3-H-shifts and cyclization to four- or five-membered rings is even tighter. The overall exothermicity in forming benzene is a strong driving force, but the intermediate steps must be successful as well. Calculations are presented here for the mechanism of Figure 1. The formation of thermal intermediates is predicted to play more of a role than in C₄H₃ and C₄H₅ additions to C₂H₂, where the low A-factors (entropic difficulty) are compensated for by low energy barriers to cyclization.

CALCULATIONAL METHODS

Multiple isomerizations require a new form of chemical-activation analysis, so we have developed¹⁸ a "Q-formalism." Some discussion of the form and nomenclature serves to clarify the process of multiple chemically activated isomerization. The *i*th isomer can be designated either as being in a specific energy state, $I_i(E)$, or as being the thermal species I_i (species in a thermal distribution). High-energy states $I_i(E)$ may be collisionally stabilized by a third-body gas, or they may decompose or isomerize unimolecularly.

Consider Figure 1. Propynyl combination forms different quantum states $I_i(E)$ of 1,5-hexadiyne ($i=1$) with a rate constant $k_{\infty}f(E, T)$, where k_{∞} is the high-pressure-limit rate constant for reactants forming the thermal adduct I_1 and $f(E, T)$ is the chemical-activation distribution function. With sufficient energy, $I_1(E)$ may:

- Be stabilized by a third-body gas M into a thermal distribution I_1 at a rate $\beta_1 Z_1 [M] \cdot [I_1(E)]$;
- Decompose to new products like $H + \dots =$ at a rate $(k_{dec}(E))_{ij} \cdot [I_i(E)]$; where j is one of $J(i)$ decomposition channels;
- Isomerize to $I_2(E)$ (1,2,4,5-hexatetraene) with a rate $(k_f(E))_i \cdot [I_i(E)]$; or
- Revert - just a decomposition channel for the first isomer, the adduct, but designated for generality as if it were a reverse isomerization with a rate of $(k_r(E))_i \cdot [I_i(E)]$.

Likewise, $I_2(E)$ may isomerize in turn to $I_3(E)$ (3,4-dimethylencyclobutene), $I_4(E)$ (fulvene), and $I_5(E)$ (benzene). Each $I_i(E)$ may be stabilized to I_i , decompose, isomerize to the next isomer, or revert to the previous isomer.

The rate constants have a compact form incorporating a recursive term Q_i . Here we show a Quantum-RRK form, where the energy variable, quantized relative to the bottom of the first energy well, is $n = E / h \langle v \rangle$:

$$k(C_3H_3 + C_3H_3 \rightarrow I_1) = \sum_{n=E/h\langle v \rangle = m_{-1}}^{\infty} \beta_1 Z_1 [M] \cdot \prod_{i=0}^n (Q_i(E)) \quad [1]$$

$$k(C_3H_3 + C_3H_3 \rightarrow P_j + P'_j) = \sum_{n=m_{-1}}^{\infty} (k_{dec}(E))_{ij} \cdot \prod_{i=0}^n (Q_i(E)) \quad [2]$$

$$Q_i(E) = \frac{k_{source}}{\beta_1 Z_1 [M] + \sum_{j=1}^{J(i)} (k_{dec}(E))_{ij} + (k_f(E))_i + (k_r(E))_i - (k_r(E))_{i+1} Q_{i+1}} \quad [3]$$

where m_{-1} is the quantized barrier for reversion of I_1 to reactants;

$k_{source} = k_{\infty}f(E, T)$ for $i=1$ or $(k_f(E))_{i-1}$ for $i>1$; and
 $(k_f(E))_i = 0$ and $(k_r(E))_{i+1} Q_{i+1} = 0$ for $i=N$.

Energy-dependent rate constants $k(E)$ for the *i*th isomer are calculated relative to the bottom of the energy well for that isomer,¹⁹ but the summations of Equation 1 and 2 are over the energies of the chemically activated adduct.

High-pressure-limit Arrhenius parameters of the different steps are the key input parameters for the calculations. Parameters in one direction are often available or may be estimated, but thermochemistry is necessary to obtain parameters in the opposite direction. Thermochemistry used here is summarized in Table I, and the resulting set of A-factors and activation energies is presented in Table II. Other parameters necessary for the calculations include mean frequency of the isomers (1010, 1240, 1176, 1209, and 1205 cm^{-1} for $i=1$ to 5, respectively); molecular weight of 78.06; Lennard-Jones parameters $\sigma = 5.27 \text{ \AA}$ and $\epsilon/\kappa = 440 \text{ K}$; and molecular weight, Lennard-Jones parameters, and collisional step-down size for the third-body gas M .

RESULTS

At high pressure (1 atm, Figure 2a) and low pressure (600 Pa, Figure 3a), C_3H_3 combination as propynyls is predicted to form the thermal adduct as its dominant channel. This result is somewhat surprising, as there is

no intrinsic energy barrier to proceeding all the way to benzene or to phenyl and H. On the other hand, while the chemically activated adduct can go over the isomerization energy barrier, entropy loss in the tight transition state is a serious limitation, as manifested in the low *A*-factor. At its lowest energy level (the ground energy of the reactants), the hot adduct has 29 kcal/mol available for isomerization, but the *A*-factor, which limits *k*(*E*), is only $3 \cdot 10^{11}$ and the energy gain in isomerization is only 1 kcal/mol. Stabilization of the adduct is then relatively easy. At higher energy levels, reached at higher temperatures, the *A*-factors favor reversion to reactants by a loose transition state. Phenyl contributes only slightly, and then only at 600 Pa and the highest temperatures; DMCB is the dominant thermal product, which may rapidly, thermally isomerize.⁵

Once 1,5-hexadiyne forms, it may isomerize thermally to benzene. Likewise, the next most important products, 1,2,4,5-hexatetraene and 3,4-dimethylcyclobutene may form benzene thermally.

Combination as propadienyls should be much less favorable. Radical density is greatest on the CH₂ group within C₃H₃, corresponding to propynyl, and C₃H₃ tends to react as propynyl.⁵ If C₃H₃ had 10% propadienyl character, the probability of propadienyl+propadienyl combination would only be 1% of the total combination rate. Again, though, thermal isomerization of the products would be possible. Also, head-to-tail combination (propynyl + propadienyl) forms 4,5-hexadienyn, which may isomerize to benzene thermally.²⁹

These results would agree with the experimental results of Alkemade and Homann³ only if thermal isomerization contributed, but there is no conflict with the C₂H₂/O₂/Ar flame data of Westmoreland et al.³⁰ The predicted rate constants would easily account for the rate of C₆H₆ production in that flame, as molecular-beam mass spectrometry does not resolve isomers of mass 78. Also in that work, a microprobe sample of the stable species was collected downstream of the region of high C₆H₆ production rate. GC/MS analysis using aDB-5 fused-silica column identified four isomers of mass 78 at concentrations of 6, 1.3, 20 (for benzene), and 0.4 ppmv in the flame. Future work in our laboratory will examine the isomer split throughout this flame.

Another possible cause of discrepancy is uncertainty in the input barriers. Stein inferred a rate constant of $8 \cdot 10^{12} \exp(-50.0/RT)$ for DMCB pyrolysis to fulvene and benzene.⁵ Using these alternative parameters for DMCB → fulvene, little change in the largest rate constants is predicted at 1 atm. In contrast, direct formation of phenyl contributes much more significantly at 600 Pa and the highest temperatures, although the thermal path is also predicted to dominate at lower temperatures. Again, having no intrinsic barrier is helpful, but entropic limitations are also very important.

ACKNOWLEDGEMENTS

This material is based upon work supported by the National Science Foundation under Grants No. CTS-88-10562 and CTS-9057406, by the Exxon Education Foundation, and by the General Electric Company. The Government has certain rights in this material.

REFERENCES

1. Wu, C.H.; Kem, R. D. *J. Phys. Chem.* **1987**, *91*, 6291.
2. Kern, R. D.; Singh, H. J.; Wu, C.H. *Int. J. Chem. Kin.* **1988**, *20*, 731.
3. Alkemade, U., and Homann, K. H. *Z. Phys. Chem. N.F.* **1989**, *161*, 19.
4. Thomas, S. D.; Westmoreland, P.R. "Role of C₃H₃ in Aromatics and Soot Formation," Paper 130g, 1989 Annual Meeting of AIChE, San Francisco CA, November 5-10, 1989; F. Communal, S.D. Thomas, and P.R. Westmoreland, "Kinetics of C₃ Routes to Aromatics Formation," Poster P40, 23rd Symp. (Intl.) on Combustion, Orléans France, July 22-27, 1990.
5. Stein, S. E. *23rd Symp. (Intl.) on Combustion*, The Combustion Institute, Pittsburgh (in press).
6. Seshadri, K. *23rd Symp. (Intl.) on Combustion*, The Combustion Institute, Pittsburgh (in press).
7. Miller, J. A.; Mellius, C. A. *Combustion and Flame* (in press); Miller, J. A.; Kee, R. J.; Westbrook, C. K. *Ann. Rev. Phys. Chem.* **1990**, *41*, 345.
8. Boyle, J.; Pfefferle, L. D. "Study of Higher Hydrocarbon Production During Methyl Acetylene and Allene Pyrolysis using Laser-Generated VUV Photoionization Detection," Paper 277f, 1990 Annual Meeting of AIChE, Chicago IL, November 11-16, 1990.
9. Hurd, C. D.; Macon, A. R.; Simon, J. I.; Levetan, R. V. *J. Am. Chem. Soc.* **1962**, *84*, 4509.
10. Tsang, W., Personal communication (1984).
11. Huntsman, W. D.; Wristers, H. J. *J. Am. Chem. Soc.* **1967**, *89*, 342; Huntsman, W. D. *Intra-Science Chem. Rept.* **1972**, *6*, 151.
12. Heffernan, M. L.; Jones, A. J. *Chem. Commun.* **1966**, *4*, 120.
13. Kent, J. E.; Jones, A. J. *Aust. J. Chem.* **1970**, *23*, 1059.
14. Hopf, H. *Angew. Chem. Int. Ed.* **1970**, *9*, 732.
15. Henry, T. J.; Bergman, R. G. *J. Am. Chem. Soc.* **1972**, *94*, 5103.
16. Gaynor, B. J.; Gilbert, R. G.; King, K. D.; Harman, P. J. *Aust. J. Chem.* **1981**, *34*, 449.

17. Honjou, N.; Pacansky, J.; Yoshimine, M. *J. Am. Chem. Soc.* **1985**, *107*, 5332.
18. Communal, F. "Plasma Measurements and Gas-Phase Kinetics in Silicon Deposition by PECVD," M.S. thesis, Chemical Engineering, U. Massachusetts (1990); Westmoreland, P. R. "Thermochemistry and kinetics of $C_2H_3+O_2$ reactions" (submitted).
19. Westmoreland, P. R.; Howard, J. B.; Longwell, J. P.; Dean, A. M. *AICHE J.* **1986**, *32*, 1971.
20. McMillen, D. F.; Golden, D. M. *Ann. Rev. Phys. Chem.* **1982**, *33*, 493.
21. Rosenstock, H.M.; Dannacher, J.; Liebman, J.F. *Radiat. Phys. Chem.* **1982**, *20*, 7.
22. Roth, W. R.; Lennartz, H.-W.; Vogel, E.; Leiendecker, M.; Oda, M. *Chem. Ber.* **1986**, *19*, 837.
23. de Brouckère, G.; Berthier, G. *Mol. Phys.* **1982**, *47*, 209.
24. Roth, W.R., Personal communication (1984), cited in NIST Standard Reference Database 25: The NIST Structures and Properties Database and Estimation Program, Version 1.0 (1991).
25. Domaille, P. J.; Kent, J. E.; O'Dwyer, M. F. *Aust. J. Chem.* **1974**, *27*, 2463.
26. Benson, S. W. *Thermochemical Kinetics, 2nd Ed.*, New York: Wiley (1976).
27. Jasinski, J. M.; Frisoli, J. K.; Moore, C. B. *J. Chem. Phys.* **1983**, *79*, 1312.
28. Ackermann, L.; Hippler, H.; Pagsberg, P.; Reihs, C.; Troe, J. *J. Phys. Chem.* **1990**, *94*, 5247.
29. Hopf, H. *Chem. Ber.* **1971**, *104*, 1499.
30. Westmoreland, P. R.; Dean, A. M.; Howard, J. B.; Longwell, J. P. *J. Phys. Chem.* **1989**, *93*, 8171.

Table I: Thermodynamic properties of species used in the analysis (1 atm standard state).

Species and structures	ΔH_f° ₂₉₈ (kcal/mol)	S° ₂₉₈ (cal/mol K)	Source
Propargyl, C_3H_3	81.4	60.6	ΔH_f° of McMillen and Golden (Ref. 20); S°_{298} estimated.
1,5-hexadiyne ()	99.0	81.3	ΔH_f° of Rosenstock et al. (Ref. 21), compared to 99.5 by group additivity; S°_{298} by group additivity.
1,2,4,5-hexatetraene ()	98.0	78.6	ΔH_f° of Rosenstock et al. (Ref. 21), compared to 94.5 by group additivity; S°_{298} by group additivity.
Dimethylenecyclobutene ()	80.4	68.4	ΔH_f° of Roth et al. (Ref. 22); S°_{298} from statistical mechanics using literature moments (Ref. 23) and frequencies assigned by analogies with fulvene.
Fulvene ()	53.5	67.9	ΔH_f° of Roth et al. (Ref. 22), compared to 45.4 by group additivity; S°_{298} from statistical mechanics using literature frequencies (Ref. 24) and moments (Ref. 23).
Benzene ()	19.8	64.3	Benson (Ref. 25).
Phenyl	78.5	69.4	ΔH_f° of McMillen and Golden (Ref. 20); S°_{298} of Benson (Ref. 25).
H-atom	52.1	27.4	Benson (Ref. 25).

Table II: High-pressure-limit rate constants for steps in the $C_3H_3 + C_3H_3$ reaction set. A -factors are in cm^3, mol, s units; E_{act} 's are in kcal/mol.

Reaction	k_{fwd}		k_{rev}		Sources
	A_{fwd}	$E_{a,fwd}$	A_{rev}	$E_{a,rev}$	
 → 2 C_3H_3	$6.6 \cdot 10^{17}$	63.2	$3.1 \cdot 10^{13}$	0.0	k_{rev} from $k(C_3H_3 + C_3H_3) = 3.4 \cdot 10^{13}$ by measurements of Alkemade and Homann (Ref. 3) assuming C_3H_3 had 90% propynyl character; k_{fwd} from K_c .
 → 	$3.0 \cdot 10^{11}$	34.4	$1.15 \cdot 10^{12}$	35.4	k_{fwd} from fit to data of Huntsman and Wristers (Ref. 11).
 → 2 C_3H_3	$2.8 \cdot 10^{16}$	64.2	$3.4 \cdot 10^{11}$	0.0	k_{rev} from $k(C_3H_3 + C_3H_3) = 3.4 \cdot 10^{13}$ by measurements of Alkemade and Homann (Ref. 3) assuming C_3H_3 had 10% propadienyl character.
 → 	$3.4 \cdot 10^{11}$	15.9	$5.8 \cdot 10^{13}$	33.5	k_{rev} by analogy to $k(\text{cyclobutene} \rightarrow 1,3\text{-butadiene})$ of Jasinski et al. (Ref. 27).
 → 	$3 \cdot 10^{13}$	66	$3.9 \cdot 10^{13}$	93.	k_{fwd} by analogy to $k(\text{fulvene} \rightarrow \text{benzene})$; see text for comparison to $8 \cdot 10^{12} \exp(-50.0/RT)$ of Stein (Ref. 5).
 → 	$3 \cdot 10^{13}$	66	$1.8 \cdot 10^{14}$	100	k_{fwd} from midrange of Arrhenius parameters of Gaynor et al. (Ref. 16).
 → H + Phenyl	$1.8 \cdot 10^{16}$	110.2	$2.2 \cdot 10^{14}$	0	k_{rev} from k_{300} of Ackermann et al. (Ref. 28).

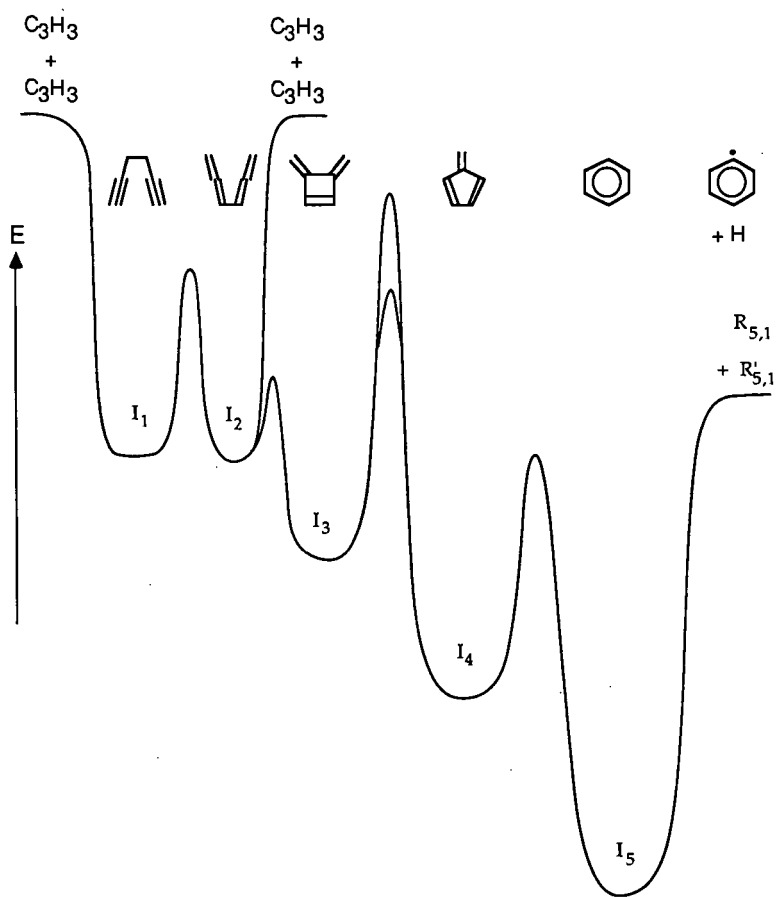


Figure 1. Energy diagram for propargyl combination, subsequent isomerizations, and decompositions.

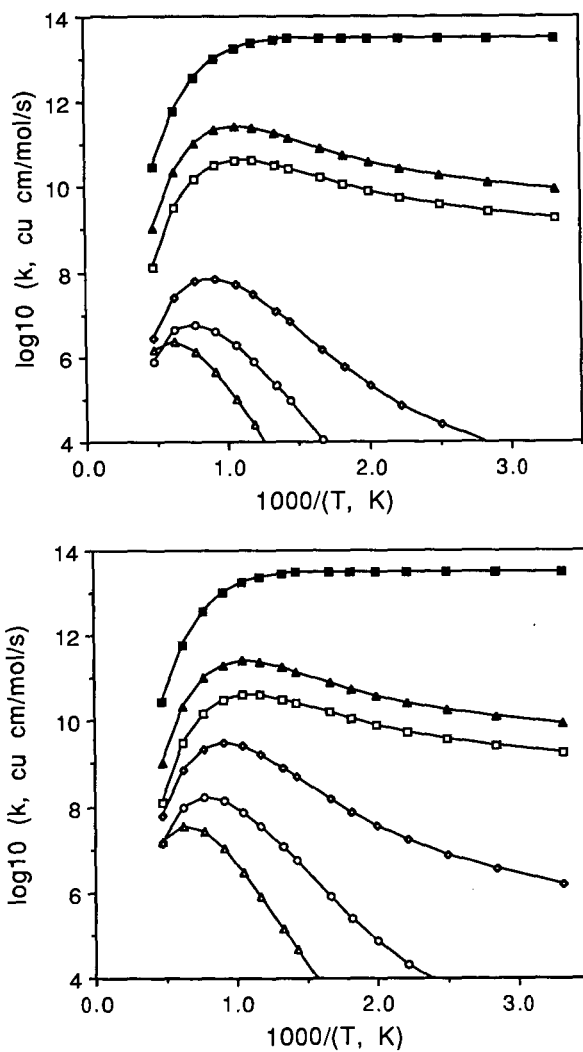


Figure 2. Arrhenius plot at 1 atm of predicted rate constants for $C_3H_3 + C_3H_3$ combining as propynyls: (top) using 66 kcal/mol barrier for DMCB to fulvene, (bottom) using 50 kcal/mol barrier of Stein (Ref. 5). Product channels: 1,5-hexadiyne ■, 1,2,4,5-hexatetraene ▲, 3,4-dimethylenecyclobutene □, fulvene ○, benzene O, H + phenyl △.

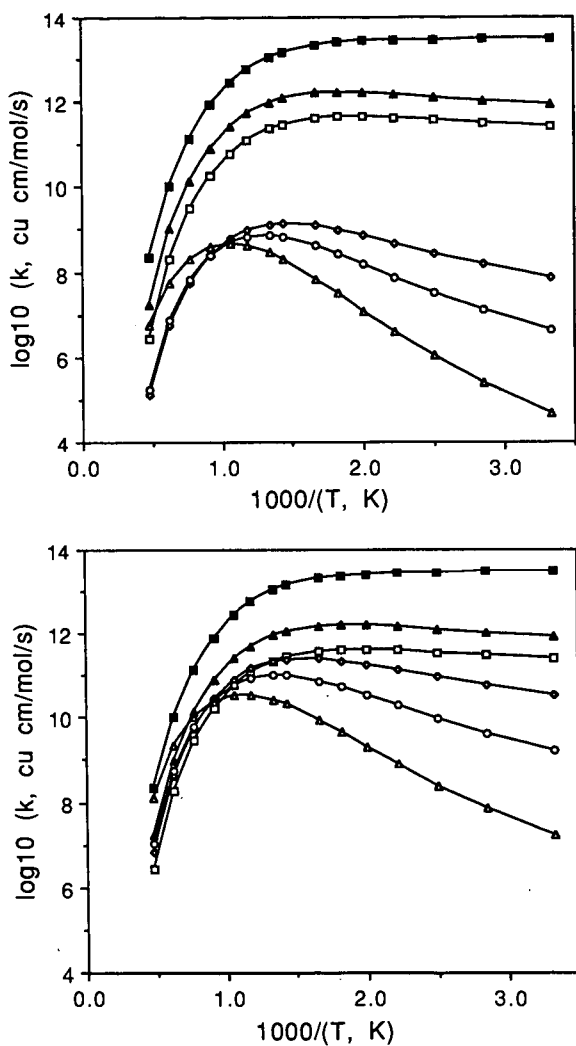


Figure 3. Arrhenius plot at 600 Pa of predicted rate constants for $\text{C}_3\text{H}_3 + \text{C}_3\text{H}_3$ combining as propynyls: (top) using 66 kcal/mol barrier for DMCB to fulvene, (bottom) using 50 kcal/mol barrier of Stein (Ref. 5). Product channels: 1,5-hexadiyne ■, 1,2,4,5-hexatetraene ▲, 3,4-dimethylenecyclobutene □, fulvene ◇, benzene ○, H + phenyl △.

COMPARISON OF AROMATICS FORMATION IN DECANE AND KEROSENE FLAMES

Christian Vovelle, Jean-Louis Delfau
Marcelline Reuillon, Robert Akrich, Mohamed Bouhria, Oumar Sanogo.
Laboratoire de Combustion et Systèmes Réactifs (LCSR-CNRS)
1C Avenue de la Recherche Scientifique
45071 ORLEANS CEDEX 2, FRANCE

Keywords : Flame Structure, Aromatics, Modelling

INTRODUCTION

Most studies on aromatics formation in flames have been concentrated on small fuel molecules¹⁻⁶. On the other hand, practical combustion systems such as automotive or airplane engines burn hydrocarbon fuels containing seven to fourteen carbon atoms. Moreover, the few kinetic studies on the combustion of liquid fuels have been oriented towards knock phenomenon and have been conducted in a temperature range (lower than 1000K) where peroxides formation dominates^{7,8}. Aromatics and soot are formed at higher temperature, and to improve knowledge on formation of these pollutants in practical systems, there is a need for experimental and modelling studies on flames of large fuel molecule.

A few years ago, we started both experimental and modelling studies on rich premixed kerosene flames. Since kerosene is a complex mixture with alkanes as major components, the structure of a near sooting decane flame (equivalence ratio 1.9) was studied first and we developed a kinetic model which predicted the mole fraction profiles of species involved in the formation of benzene with a good accuracy⁹.

In this work we present the result of temperature and mole fraction measurements in sooting kerosene and decane flames. Results show that for all species except benzene there is a close similarity between the two flames so that the kinetic mechanism derived for decane is also valid for modelling kerosene combustion with only one change concerning benzene formation. A specific study was carried out to identify an additional source for aromatics formation in kerosene flames.

EXPERIMENTAL

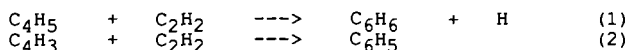
The premixed sooting kerosene flame (8.0% kerosene, 56.4% oxygen, 35.6% argon) was stabilized on a flat flame burner at low pressure (6 kPa). If kerosene was decane, this corresponds to an equivalence ratio of 2.2. Gas velocity at burner exit was 24 cm/s. A decane-O₂-Ar flame with the same initial composition was stabilized and analyzed in identical conditions. Temperature and mole fraction profiles were measured along the symmetry axis. Molecular beam mass spectrometry technique was used for species analysis and Pt-Pt 10% Rh thermocouples for temperature measurements (wires diameter 50 μ m). Coating with BeO/Y₂O₃ prevented catalytic effects, and heat losses due to radiation were compensated by electrical heating. Identification of species and calibration of the mass spectrometer have been described elsewhere^{10,11}.

A Gilson pump manufactured for Liquid Chromatography was used to control the flow rate of kerosene. The fuel was first atomized by dragging through a small orifice by a high pressure argon jet and then

vaporized in a heated chamber. Adjustment of atomizer and vaporizer temperature was rather critical. Temperature had to be maintained between 170°C and 200°C to prevent fuel condensation or polymerization, respectively.

RESULTS

In a previous study on the modelling of acetylene flames, the formation of the first aromatic rings was described by acetylene addition to C₄ species :



Kinetic parameters for these reactions were taken from Westmoreland¹². The mechanism for rich decane flames was built upon addition to the acetylene mechanism of a few reactions for decane consumption⁹. The ability of the mechanism to predict aromatic formation depends strongly on the accuracy of the modelling of C₄ species and their precursors : C₂H₄ and C₂H₂. Maximum mole fraction measured for the major molecular and active species, and for the species involved in aromatics formation, in the kerosene and decane flames have been compared in Table I.

Slight differences are observed for some species. They were not considered as significant but rather due to a lower accuracy of the measurements in the kerosene flame where very low electron energies were used to prevent fragmentations of the fuel components. However the maximum mole fraction for benzene in the kerosene flame exceeds by one order of magnitude the maximum measured in the decane flame.

This point deserved attention and a specific comparative study on the formation of benzene and two others aromatic species : phenyl acetylene and vinyl benzene in decane and kerosene flames was undertaken. To check the possibility of a change in the mechanism for aromatics formation described above, acetylene was measured as well.

Aromatics formation in kerosene and decane flames

Detailed analysis of the structure of one flame is time-consuming and this study was limited to signal measurements. On the other hand, they were repeated for many flames with equivalence ratio in the range 1.0 - 2.5. Change in fuel composition have been done keeping constant both the overall and the argon flowrates. Gas velocity at the burner exit was 27.5 cm/s (at 298K and 6.0 kPa).

Figure 1 shows that the maximum mole fraction of acetylene in decane flames is slightly greater than in kerosene flames. In both flames, a linear increase is observed for equivalence ratios above 1.6.

Benzene measurements have been performed with an electron energy adjusted to 13 eV. For kerosene flames a second determination has been done with an electron energy of 11 eV to check the occurrence of fragmentations in the ionization source of the mass spectrometer. A similar result (linear variation of the maximum signal with the equivalence ratio) is obtained in both cases, so that we can conclude that measurements of the benzene signal are free from fragmentation

effects (Figure 2). Extrapolation of the signal gives a null value for an equivalence ratio equal to 0.8.

Measurements in the decane flame confirm that benzene is formed in lower concentration than in kerosene flames. The ratio is about 10 for an equivalence ratio of 2.0. A second difference with kerosene flames is observed for the variation of the maximum signal with the equivalence ratio, the exponent in a law $[C_6H_6] = f(\phi)$ being greater than 1.

The curves plotted in figure 2 show that benzene formation results from two different mechanism in decane and kerosene flames. In the former, benzene is formed by reactions (1) and (2) so that the signal is proportional to acetylene and either C_4H_3 or C_4H_5 . Since in turn, C_4 species are formed from acetylene, benzene dependence with $[C_2H_2]^2$ must be observed. The dashed line in figure 2 corresponds to the variation with ϕ of the expression $k[C_2H_2]^2$ with the constant k adjusted so that the value calculated for $\phi = 2.4$ coincide with the signal measured for benzene. These two curves remains very close over the whole range of equivalence ratios. ($[C_2H_2]$ represents the maximum signal measured for acetylene).

In kerosene flames, the linear variation of the benzene signal with $(\phi - \phi_c)$ shows that the aromatics components of the fuel contribute directly to benzene formation. The procedure adopted to change the equivalence ratio of the flames (constant values of overall an argon flowrates) leads to the following relationship between decane flowrate and ϕ :

$$F_d = (F_o - F_{Ar}) \frac{2(\phi - \phi_c)}{2(\phi - \phi_c) + 31}$$

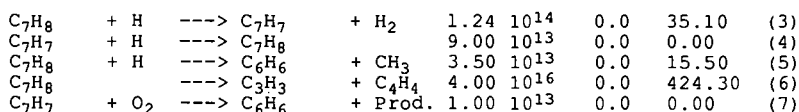
(F_d , F_o , F_{Ar} represents respectively decane, overall and argon flowrates).

Since $2(\phi - \phi_c)$ is small compare to 31, this expression predicts a linear variation for F_d with $(\phi - \phi_c)$

Phenyl acetylene and vinyl benzene signals correspond as well to different sources for aromatics. In decane flames, these two species are not observed for equivalence ratios lower than 1.5, while a marked increase in the signal is observed for richer flames (Figure 3). Since these species are formed by addition of acetylene to benzene or phenyl radical we have plotted the variation of the expression $k[C_6H_6][C_2H_2]$ versus ϕ . Here again, the value of the constant k was arbitrarily adjusted in order to match either the phenyl acetylene or the vinyl benzene signal at $\phi = 2.4$. The same comparison in kerosene flames leads to values derived from $[C_6H_6]$ and $[C_2H_2]$ lower than the experimental signal when ϕ is close to 1.0 (Figure 4). Expressions based on the product of the reactants signals give only an upper limit for the formation of a given species since consumption is not taken into account. Therefore, from the relative positions of the experimental points and the dashed curve, we can conclude that phenyl acetylene and vinyl benzene measured in stoichiometric or slightly rich kerosene flames result from the aromatic components of the fuel.

Benzene formation in kerosene flames

This comparative study clearly shows that consumption reactions of at least one aromatic species must be added to the decane mechanism to predict the structure of rich kerosene flames. Tri-methylbenzene is the main aromatic species in the kerosene that was used in this work. However, to simplify both the mechanism and the search for kinetic data, the aromatic part of kerosene was considered as toluene and the following reactions were considered to describe its consumption :



Kinetic data for these reactions have been taken from Rao and Skinner¹³.

Modelling of kerosene flames

These five reactions have been added to the mechanism validated previously for decane combustion⁹. Simulation of the kerosene flame has been performed with a fuel composition of 10% toluene and 90% decane. Warnatz's computation code was used with the experimental temperature profile as input data, so that the energy equation was neglected. Temperature profiles were measured by moving the burner in the vertical direction. The thermocouple was kept at a fixed position, close to the quartz cone tip, in order to take into account flame perturbation by the cone. The measurements have been repeated for various distance (d) between the thermocouple bead and the cone tip (Figure 5). In the burned gases only a cooling effect is observed, while in the main reaction zone, flame attachment shifts the profiles towards larger distance from the burner surface. No one profile is representative of the gas sampling conditions in the whole flame : profiles with very small d correspond to the temperature evolution for sampling close to the burner surface, while profiles with large d give a better description of the temperature history for a gas sample taken far from the burner. In this work, the profile measured with d = 3 mm was chosen as the best compromise between these extreme situations.

The SANDIA thermodynamic data base¹⁴ has been used for species involved in H_2 , C_1 and C_2 submechanisms and Burcat's data¹⁵ for decane and toluene combustion reactions.

Simulated mole fraction profiles are compared to the experimental ones for the reactants, the main products, and species involved in the formation of aromatics from the alkane part of the fuel (Fig. 6-9). In figure 10, prediction of the mole fraction profile is compared to experimental results for a decane and a kerosene flame. This figure shows that in the latter, benzene results mainly from the aromatic part of the fuel. This contribution can be modelled with a good accuracy by addition to the mechanism of a few reactions for the consumption of one aromatic.

CONCLUSION

This work was concerned with the formation of aromatics in kerosene flames. In previous studies we checked the possibility to substitute decane to kerosene to perform modelling in simpler conditions. Results showed that structure of decane and kerosene flames are similar except

for benzene that is formed in larger amount in kerosene flames. A specific study based on the systematic measurement of acetylene, benzene, phenyl acetylene and vinyl benzene in decane and kerosene flames was carried out. Variation of the maximum signal with the equivalence ratio leads to the conclusion that the aromatic part of kerosene is the main source of aromatics, while it is the addition of acetylene to C4 radicals in the decane flame. This difference was taken into account by addition of a few reactions for the consumption of toluene to the decane combustion mechanism used so far. This change leads to predictions in good agreement with the experimental mole fraction profiles in decane and kerosene flames.

REFERENCE

1. MILLER, J.A., MITCHELL, R.E., SMOOKE, M.D. and KEE, R.J., Nineteenth Symposium (International) on Combustion, p. 181, The Combustion Institute, (1988).
2. WESTBROOK, C.K. and DRYER, F.L., *Progr. Energy Comb. Sci.* 10, 1 (1984).
3. WARNATZ, J. *Comb. Sci. Tech.* 34, 177 (1983).
4. WESTMORELAND, P.R., HOWARD, J.B. and LONGWELL, J.P., Twenty First Symposium (International) on Combustion, p. 773, The Combustion Institute, (1988).
5. FRENKLACH, M. and WARNATZ, J., *Comb. Sci. and Tech.* 51, 265 (1987).
6. HARRIS, S.J., WEINER, A.M. and BLINT, R.J., *Comb. and Flame*, 72, 91, (1988).
7. AXELSSON, E., BREZINSKY, K., DRYER, F.L., PITZ, W.J. and WESTBROOK, C.K., Twenty First Symposium (International) on Combustion, p. 783, The Combustion Institute, (1986).
8. WESTBROOK, C.K., WARNATZ, J. and PITZ, W.J., Twenty Second Symposium (International) on Combustion, p.893, The Combustion Institute, (1988).
9. DELFAU, J.L., BOUHRIA, M., REUILLON, M., SANOGO, O., AKRICH, R. and VOVELLE, C., Twenty Third Symposium (International) on Combustion, The Combustion Institute, (1990).
10. BASTIN, E., DELFAU, J.L., REUILLON, M., VOVELLE, C. and WARNATZ, J., Twenty Second Symposium (International) on Combustion, p. 313, The Combustion Institute, (1988).
11. BASTIN, E., Thèse de Doctorat de l'Université Pierre et Marie Curie (Paris 6), Spécialité Cinétique Chimique Appliquée (1989).
12. WESTMORELAND, P.R., DEAN, A.M., HOWARD, J.B. and LONGWELL, J.P., *J. Phys. Chem.*, 93, 8171 (1989).
13. RAO, V.S. and SKINNER, G.B., *J. Phys. Chem.*, 88, 4362-4365, (1984).
14. KEE, R.J., RUPLEY, M. and MILLER, J.A., The Chemkin Thermodynamic Data base, SANDIA Report, SAND87-8215-UC-4 (1987).
15. BURCAT, A., Table of Coefficients Sets for NASA Polynomials, Appendix C, in *Combustion Chemistry*, (Gardiner, W.C. Jr. Ed.), Springer-Verlag, New York, (1984).

	Decane-O ₂ -Ar flame	Kerosene-O ₂ -Ar flame
CO	3.4 10 ⁻¹	2.9 10 ⁻¹
H ₂ O	3.0 10 ⁻¹	2.4 10 ⁻¹
H ₂	2.3 10 ⁻¹	3.0 10 ⁻¹
CO ₂	6.0 10 ⁻²	7.0 10 ⁻²
H	8.9 10 ⁻³	1.2 10 ⁻³
OH	2.7 10 ⁻⁴	3.7 10 ⁻⁴
C ₂ H ₄	5.3 10 ⁻²	1.7 10 ⁻²
C ₂ H ₂	6.1 10 ⁻²	3.9 10 ⁻²
C ₄ H ₂	1.4 10 ⁻³	1.8 10 ⁻³
C ₄ H ₄	5.9 10 ⁻⁴	1.1 10 ⁻³
C ₄ H ₅	3.3 10 ⁻⁵	1.0 10 ⁻⁴
C ₆ H ₆	1.2 10 ⁻⁴	2.2 10 ⁻³

Table I

Comparison of the maximum mole fraction in decane and kerosene flames (equivalence ratio : 2.2, pressure : 6 kPa).

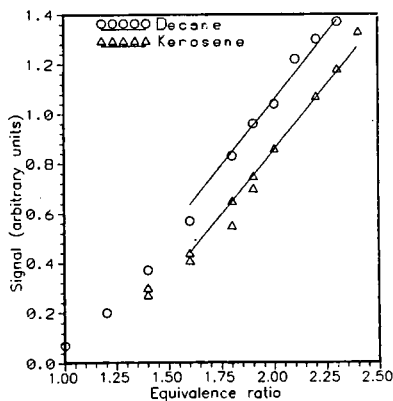


Figure 1
Evolution with the equivalence ratio of the maximum signal of C₂H₂

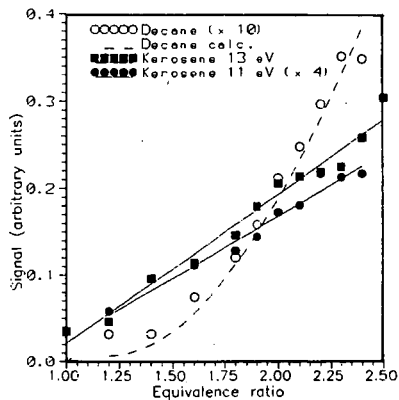


Figure 2
Evolution with the equivalence ratio of the maximum signal of C₆H₆

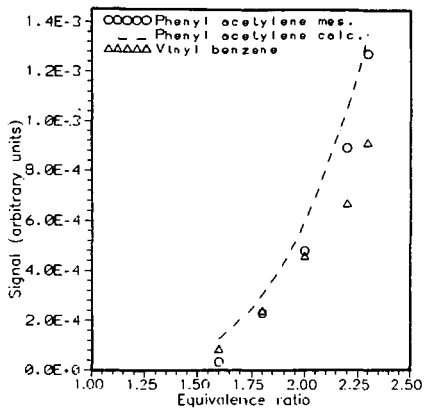


Figure 3
Decane flames

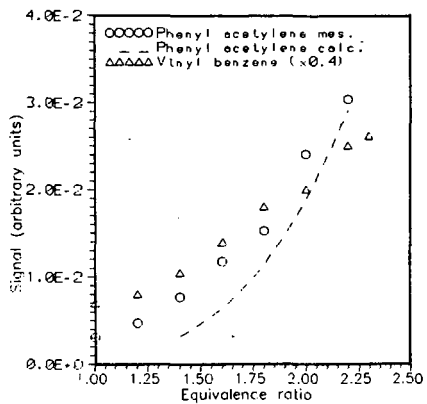


Figure 4
Kerosene flames

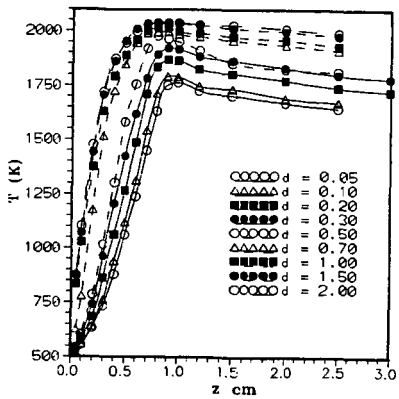


Figure 5
Temperature profiles
in a $\varnothing = 2.2$ Kerosene- O_2 -Ar flame

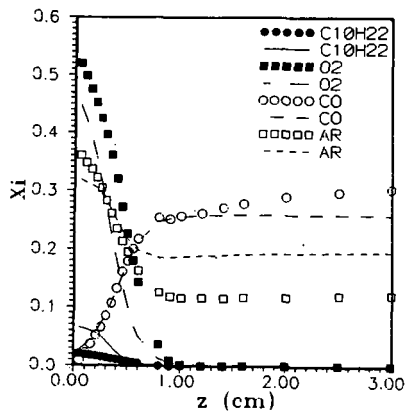


Figure 6
Comparison of experimental (points)
and simulated (curves)
mole fraction profiles
 $\varnothing = 2.2$ Kerosene- O_2 -Ar flame

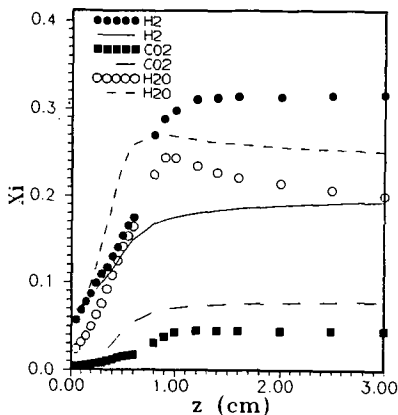


Figure 7
Comparison of experimental (points)
and simulated (curves)
mole fraction profiles
 $\phi = 2.2$ Kerosene- O_2 -Ar flame

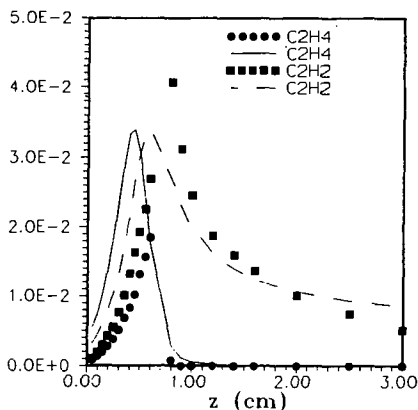


Figure 8
Comparison of experimental (points)
and simulated (curves)
mole fraction profiles
 $\phi = 2.2$ Kerosene- O_2 -Ar flame

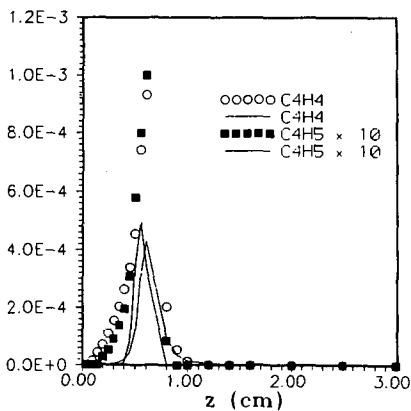


Figure 9
Comparison of experimental (points)
and simulated (curves)
mole fraction profiles
 $\phi = 2.2$ Kerosene- O_2 -Ar flame

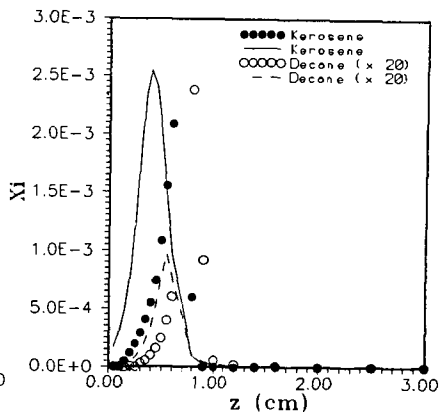


Figure 10
Comparison of experimental (points)
and simulated (curves)
mole fraction profiles
 $\phi = 2.2$ Decane and Kerosene flames

REACTION RATES OF A FEW BENZYL TYPE RADICALS WITH O₂, NO AND NO₂

J.F. Pauwels, L. El Maimouni, A. Goumri, P. Devolder, L.R. Sochet

Laboratoire de Cinétique et Chimie de la Combustion
URA CNRS 876
59655 VILLENEUVE D'ASCQ Cédex (France)

keywords : rates of elementary reactions-substituted benzyl radicals - reactions with O₂, NO, NO₂

Introduction

Benzyl type radicals are important conjugated intermediates in the chemical mechanisms describing the oxidation of alkylbenzenes in reactive systems. In the atmosphere, they are formed during the first step (by OH abstraction) of the tropospheric oxidation of alkylbenzene derivatives (toluene, xylenes, trimethylbenzenes) : final oxidation are formed by subsequent competing reactions of the benzyl type radicals with O₂, NO and NO₂ (1) (2). In high temperature reactive systems, they can also play a role as intermediates in the mechanism of soot formation (3) (4) (5) (6). At last, with the allyl radical, the benzyl radical is a reference conjugated radical. With an absolute technique, the discharge flow/Laser Induced Fluorescence technique, we have measured the room temperature rate constants with O₂, NO and NO₂ of the following benzyl type radicals : m-fluorobenzyl, p-fluorobenzyl, o-methylbenzyl, m-methylbenzyl. Also, the rate constant with O₂ of the p-fluorobenzyl radical has been measured in the temperature range 297-433 K.

Experimental

A schematics of the experimental set up is presented figure 1. The radicals are formed by chlorine atom reaction with the parent molecule as a precursor. Chlorine atoms are prepared in the upstream part of the flow tube by the fast reaction of transfer (7) :



with F atoms first produced by a microwave discharge in F₂/He or CF₄/He. This method (chlorine abstraction) has been preferred to the more direct fluorine abstraction because (i) a significant fraction of fluorine atoms exhibit an addition on the aromatic ring (8) (9) (ii) chlorine abstraction is a very fast reaction ($k = 6 \times 10^{-10} \text{ cm}^3 \text{ molec}^{-1} \text{ s}^{-1}$ (10)). The precursor and the reactant (O₂, NO or NO₂) are then successively added via a double movable injector. The benzyl type radicals are probed by Laser Induced Fluorescence via their visible absorption bands ($\lambda \sim 460 \text{ nm}$) which have been characterized in gas phase either as absorption bands (13) or as fluorescence excitation bands (11) (12). The exciting wavelength ($\lambda \sim 460 \text{ nm}$) is generated by a dye laser (Rhodamine 590) pumped by a Yag laser (both Quantel) and further blueshifted (generation of the first Anti-Stokes harmonics) via a Raman cell (14). The fluorescent light is filtered by an interference filter ($\lambda = (500 \pm 20) \text{ nm}$) and averaged by a boxcar (PAR 162/165).

For the room temperature measurements, both the flow tube and the injector are covered with a halocarbon, wax whereas for variable temperature measurements, all flow surfaces are simply washed with HF. Most experiments have been performed at a pressure of 1 torr with Helium as diluent gas. O₂ (Alphagaz N45, 99.995%) is used as received. NO₂ is purified as follows : to oxidize the other nitrogen oxides usually present

in NO₂ (bluish color at 77 K), liquid NO₂ is first placed under ultrapure oxygen during ~ 24 hours and then submitted to extensive degassing at 77 K. Traces of NO₂ present in NO (Alphagaz N20, 99%) have been eliminated by flowing NO through a combination of charcoal filter and a filter packed with FeSO₄, 7H₂O (15).

Results and discussion

1) Rate constants of a few benzyl type radicals with O₂, NO and NO₂.

A few typical curves observed with the p-fluorobenzyl radical as an example are presented figure 2 : fig 2a represents a few logarithmic decay plots of radical concentration versus reaction distance ; fig 2b represents all the pseudo-first-order constants versus the reactant concentration. Our global results are presented table 1 together with the few other measurements available in the literature for the benzyl radical itself ; the rate constant of the benzyl radical with O₂ has already been measured by flash photolysis (16), laser photolysis/Laser Induced Fluorescence (17) and mass spectrometry (18). Our results for the substituted benzyl radicals show that the reaction rate with O₂ is not very dependent upon the presence of a substituent ; the same conclusion has been observed in liquid phase (19) for a few benzyl radicals substituted in para position by a methyl group or a fluorine atom. Furthermore, since the reaction rate constants with O₂ and NO measured with the present technique (Pressure ~ 1 torr) are very close to those measured by flash photolysis (~160 torr) (16), this suggests that these reactions have already reached their high pressure limiting values (k_{∞}) at pressures in the torr range.

2) Variable temperature measurements

The rate constant with O₂ of the p-fluorobenzyl radical, considered as a model for the benzyl radical, has been measured in the range 297-433 K. Preliminary measurements indicate a strong negative temperature coefficient, in agreement with the following Arrhenius expression :

$$k = 4 \times 10^{-15} \exp(1590/T) \text{ cm}^3 \text{ molec}^{-1} \text{ s}^{-1}$$

This expression disagrees with the absence of any variation observed by Laser photolysis/Laser Induced Fluorescence (17) in the range 295-373 K ; however, it is in agreement with the lack of reactivity of benzyl with O₂ noticed by Troe et al (20) in their shock tube investigations ; furthermore, a few negative temperature coefficients have also been reported for the following (R° + O₂ → products) reaction rates : R° = neopentyl (21), R° = ethyl (at constant [M]) (22), R° = i-C₄H₉ (23).

REFERENCES

- (1) R. Atkinson, Chem. Rev. 85 (1986) p. 69
- (2) R. Atkinson, J. Phys. and Chemical Reference data, Monograph n° 1 (1989)
- (3) K. Brozinski, G.T. Linderis, T.A. Litzinger and I. Glassman
21 st Symp. (int) on combustion (1986) p. 833
- (4) R.R. Baldwin, M. Scott, R.W. Walker
21 st Symp. (int) on combustion (1986) p.991
- (5) V.S. Rao, G.B. Skinner
21 st Symp. (int) on combustion (1986) p. 809
- (6) W. Müller-Markgraf and J. Troe
21 st Symp. (int) on combustion (1986) p. 815
- (7) J.J. Schwab and J.G. Anderson, J. Quant. Spectros.
Radiative transfer 27 (1982) 445
- (8) M.A. Hoffbauer and J.W. Hudgens, J. Phys. Chem. 89 (1985) 5152

- (9) J. Ebrecht, W. Hack, H. Gg. Wagner, *Berichte Bunsenges Phys. Chem.* 93 (1989) 619
 (10) M. Bartels, J. Edelbüttel-Einhaus, K. Hoyerman, 22nd Symp. (int) on combustion, Seattle (1988) 1041
 (11) M. Fukushima, K. Obi, *J. Chem. Phys.* 93 (1990) 8488
 (12) T.R. Charlton, B.A. Trush, *Chem. Phys. Lett.* 125 (1986) 547
 (13) T.F. Bindley, A.T. Watts, S. Walker, *Trans. Faraday Soc.* 60 (1964) 1
 (14) U. Wilke, W. Schmidt, *Opt. Comm.* 19 (1976) 116
 (15) G. Helas, M. Flanz, P. Warneck, *Intern. J. Environ. Anal. Chem.* 10 (1981) 155
 (16) T. Ebata, K. Obi, I. Tanaka, *Chem. Phys. Lett.* 77 (1981) 480
 (17) H.H. Nelson, J.R. McDonald, *J. Phys. Chem.* 86 (1982) 1242
 (18) M. Bartels, J. Edelbüttel-Einhaus, K. Hoyermann
 Proceedings of the 22th Symposium on combustion (1988) 1041
 (19) K. Tokumara, H. Nosaka, T. Ozaki, *Chem. Phys. Lett.* 169 (1990) 321
 (20) H. Hippler, J. Troe
 23rd (int) symposium on combustion, Orléans (1990) paper n° 55 p. 28
 (21) Z. Xi, W-J Han, K.D. Bayes
J. Phys. Chem. 92 (1988) 3450
 (22) A.F. Wagner, I.R. Slagle, D. Sarzynski, D. Gutman
J. Phys. Chem. 94 (1990) 1854
 (23) I.R. Slagle, J.R. Bernhardt, D. Gutman
 22nd (int) Symp. combustion (1988) p. 953

Radical	Reactant			Ref
	O ₂	NO	NO ₂	
benzyl	0.99	9.5		(16)
	1.5			(17)
	> 0.5			(18)
p-fluorobenzyl	0.82	10	49	this work
m-fluorobenzyl	0.6	9	48	this work
o-methylbenzyl	1.2	9.4	50	this work
o-methylbenzyl	1.2	8.6		(16)
m-methylbenzyl	1.1	13	60	this work

Table 1 : rate constants of benzyl and substituted benzyl radicals (in $10^{-12} \text{ cm}^3 \text{ molec}^{-1} \text{ s}^{-1}$)

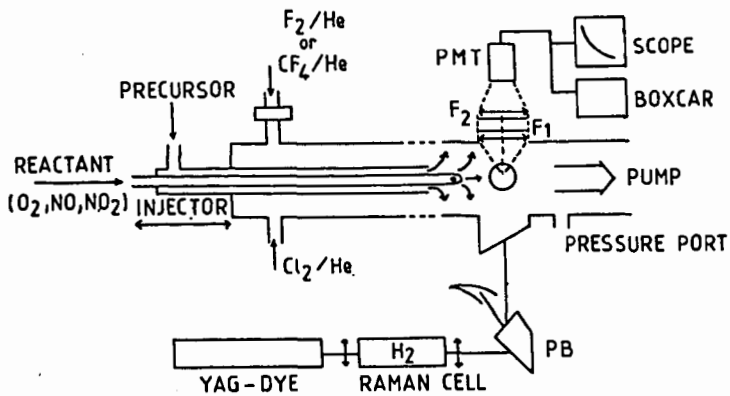


FIG. 1
SCHEMATIC OF THE EXPERIMENTAL SET-UP

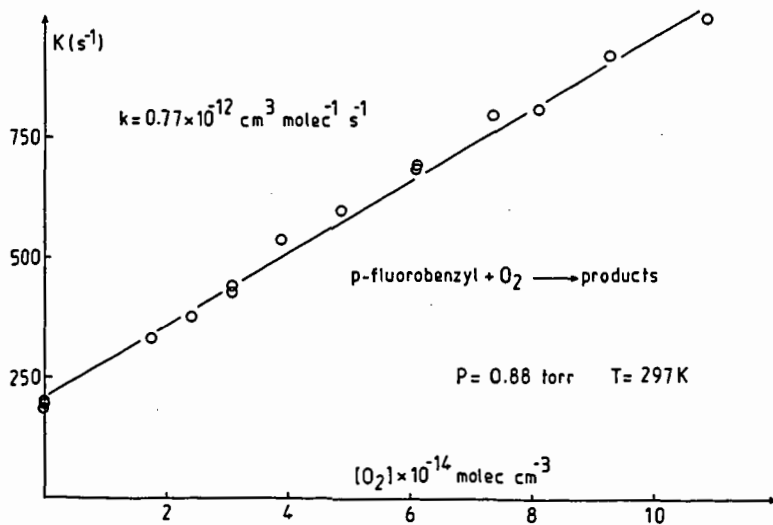


FIG. 2b: PSEUDO-FIRST-ORDER RATE CONSTANTS ($K(s^{-1})$)
VERSUS OXYGEN CONCENTRATION

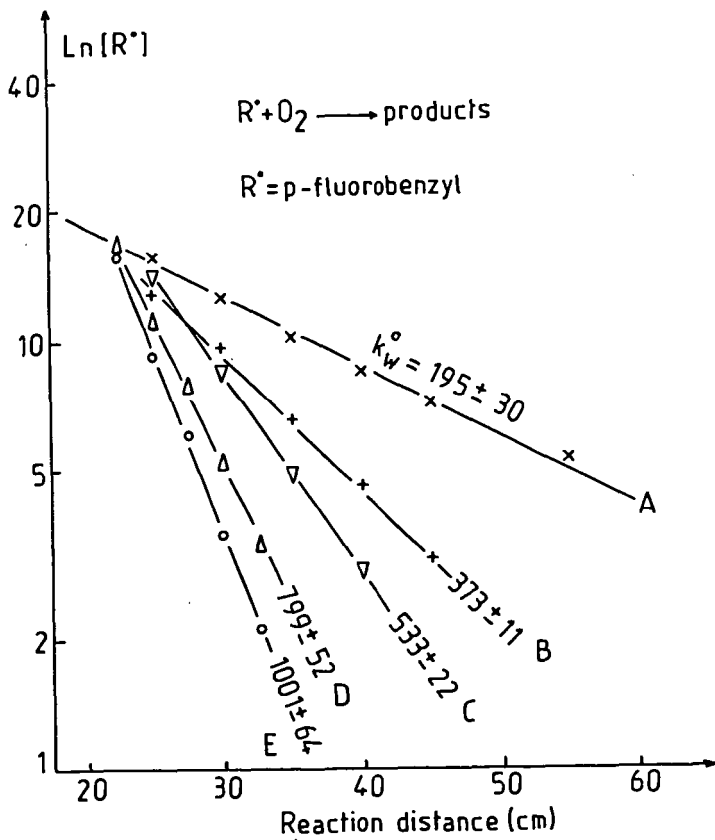


FIG 2a: RADICAL DECAY PLOTS VERSUS INJECTOR DISPLACEMENT
 (REACTION DISTANCE) FOR VARIOUS OXYGEN CONCENTRATIONS
 (in 10^{14} molec cm^{-3}): A(0), B(2.42), C(4.27), D(7.43)
 E(10.9); THE CORRESPONDING SLOPES ARE IN s^{-1}

KINETICS OF REACTIONS OF PROTOTYPICAL AROMATIC HYDROCARBONS
WITH O (³P) ATOMS AND CH₂ (\bar{X} ³B₁) RADICALS: A COMPARATIVE STUDY

F. Temps and H. Gg. Wagner
Max-Planck-Institut für Strömungsforschung, Bunsenstrasse 10,
3400 Göttingen, Germany

Keywords: Aromatics, kinetics, methylene radicals, oxygen atoms.

INTRODUCTION

Mono- and polycyclic aromatic hydrocarbons constitute important intermediates and by-products of technical combustion processes (see, e.g., [1]). Their build-up and subsequent fate is well appreciated to be critically determined by reactions with small, highly reactive O- or C-containing radicals. However, despite their importance, the detailed mechanisms and kinetics of the distinctive elementary reactions which can take place still present many questions. In the present paper we consider reactions of selected aromatic hydrocarbons with two particularly interesting free radicals, namely O (³P) (\equiv ³O) and CH₂ (\bar{X} ³B₁) (\equiv ³CH₂). While O is an important oxidizing species, CH₂ as the most abundant highly reactive C-centered small radical in flames can contribute to the build-up of larger molecules by adding reactive side groups to a substrate. Recent experimental results for the kinetics of both species with prototypical unsubstituted mono- and polycyclic aromatics as well as simple alkyl substituted derivatives are summarized. Reactants include benzene, naphthalene, phenanthrene, toluene, ethylbenzene, and cumene. The investigations were motivated by the desire to find some simple correlations which would help to estimate rate parameters for ³O or ³CH₂ with other reactants for which experiments cannot be performed easily. Thus, the focus is on a critical comparison of the chemical reactivities of the two radicals, which since they are isoelectronic are expected to exhibit parallel reactivities. Analogies have been observed concerning addition reactions to the aromatics. On the other hand, H atom abstraction from alkyl side chains could only be observed for ³CH₂ but seems to play little role for ³O. A difference with dramatic importance to combustion processes arises as a consequence of the low singlet-triplet splitting between CH₂ (\bar{X}) and CH₂ (\bar{a} ¹A₁) (\equiv ¹CH₂), $\Delta H_0^\ddagger = 37.7$ kJ/mol [2].

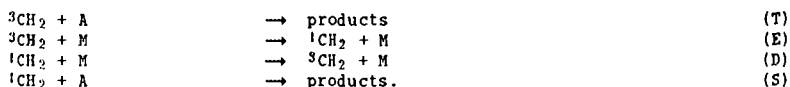
EXPERIMENTAL

Experimental studies of reactions of ³O and ³CH₂ with aromatics A have been performed using the discharge flow technique. Experimental set-ups have been described [3a, 4]. Reactions of ³O atoms were studied in the temperature range 300 K \leq T \leq 880 K under pseudo-first-order conditions with [O] \gg [A]. Absolute O concentrations were determined using the titration reaction N + NO. Concentration-versus-time profiles of O and A were followed by mass spectrometry. The reactions of ³O with benzene and toluene were also investigated using the shock tube technique [3e-f]. Reactions of ³CH₂ were studied in the temperature range 360 K \leq T \leq 700 K under conditions [A] \gg [³CH₂] with Laser Magnetic Resonance (LMR) detection of ³CH₂. The reaction O + CH₂CO \rightarrow CH₂ + CO₂ served as the radical source. Reaction product were determined by GC or GC-MS analysis after photolyzing CH₂CO at either $\lambda_1=366$ or $\lambda_2=312$ nm in a static cell in the presence of reactants A [5a]. CH₂CO photodissociation at these wavelengths yields practically only ³CH₂ or ¹CH₂, respectively [6].

RESULTS AND DISCUSSION

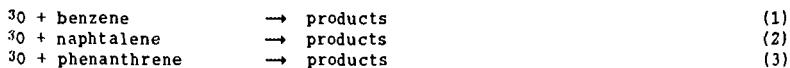
The rate coefficients for the reactions of ^3O with reactants A can be determined directly from the pseudo-first-order decay plots of [A] and the known O concentrations. Performing experiments under the condition $[\text{O}] \gg [\text{A}]$ has the advantage that heterogeneous processes and consecutive reactions of the various products can hardly affect the kinetic results. ^1O atoms play no role in thermal systems.

Data analysis for the reactions of $^3\text{CH}_2$ is somewhat more involved. Rate constants obtained from pseudo-first-order decay plots of $[\text{CH}_2]$ in the absence and presence of a large excess of [A] refer to the total depletion of $^3\text{CH}_2$ via all possible pathways [7]. In the first place one has the reactive channels (T) of $^3\text{CH}_2$ with the substrates. However, because of the small singlet-triplet splitting, partial thermal equilibration (E/D) with collision partners M between the two CH_2 electronic states has to be taken into account as well. $^1\text{CH}_2$ undergoes very fast consecutive reactions (S) with the reactants:



With the steady state assumption for $^1\text{CH}_2$, the rate coefficients for deactivation and reaction of $^1\text{CH}_2$ taken from independent measurements [8] and the rate for $^3\text{CH}_2$ excitation from the equilibrium constant for $^3\text{CH}_2 \rightleftharpoons ^1\text{CH}_2$, the experimental, directly measured effective rate constants can be separated to determine the rate coefficients for the $^3\text{CH}_2$ reactive channels (T) [5d, 7].

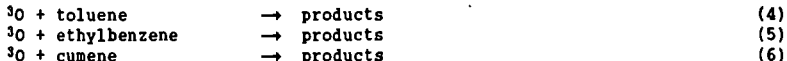
REACTIONS OF ^3O WITH UNSUBSTITUTED AROMATICS: The rate constants for the reactions of ^3O with the mono- and polycyclic unsubstituted aromatic hydrocarbons



are shown as a function of temperature in Fig. 1. Data points are from [3a-e]. Results for reaction (1) obtained in other laboratories (for references see [3a]) are in good agreement. Table 1 summarizes the Arrhenius parameters. The reactions can be seen to exhibit moderate activation energies. In accordance with theoretical expectations [9] benzene is the least reactive molecule. Naphtalene and phenanthrene behave very similarly. It is pointed out that the data for reactions (1) - (3) are in line with results for related molecules such as halogenbenzenes and pyridine [3i-j], which are less reactive than benzene, and biphenyl [3d], which reacts somewhat faster. Furthermore, in view of the different electron configurations the reaction with anthracene is expected to be significantly faster than the one with phenanthrene.

The reactions of ^3O with these aromatics proceed via addition to the ring systems yielding a triplet biradical as primary product. However, intersystem crossing to the singlet state is likely to be fast, and different isomerization and fragmentation reactions can also take place. The most exothermic reaction channels are those leading to phenols, which at high pressures can be collisionally stabilized. Formation of a seven-membered ring containing the O atom or of corresponding "epoxy" isomers are other possibilities. In the low pressure regime H elimination to yield phenoxy type radicals has been observed, while elimination of CO has been concluded to be of minor importance [10a]. H atom abstraction by ^3O from the aromatic ring is endothermic and has a high activation energy. Its role under flame conditions can be estimated from an Evans-Polanyi plot.

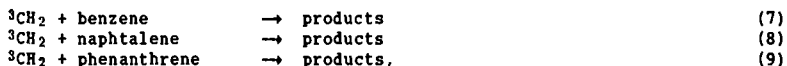
REACTIONS OF ^3O WITH ALKYL SUBSTITUTED AROMATICS: Compared to the unsubstituted aromatics discussed above, alkyl substituted derivatives stand out for their two reactive centers, the aromatic ring and the side chain. The measured activation energies and preexponential factors for the selected reactions



are given in Table 1. Experiments have been described in some detail in [3a, f, h]. Reaction (4) has also been studied in several laboratories (for references see [3a]), the different results being in good agreement with each other. The overall rate constants $k_4(T) - k_6(T)$ and, for comparison, $k_1(T)$ are plotted in Figure 2. Considering the overall body of data it is apparent that the kinetics of the reactions of ^3O with benzene derivatives containing a single alkyl group are virtually identical under the conditions used. The reactions are somewhat faster than with benzene. However, there is little if any dependence on the nature of the alkyl chain (methyl vs. ethyl vs. isopropyl). Data for xylenes [3h] indicate that a second alkyl substituent leads to some further acceleration of the reaction.

Concerning the reaction mechanism, the question arises whether the main reaction channels involve attack by ^3O of the aromatic ring or of the alkyl group. Because of the weak benzylic C-H bonds (e.g., $\Delta H_{298}[\text{H}-\text{CH}_2\text{C}_6\text{H}_5] = 378 \text{ kJ/mol}$ [11]) H atom abstraction from these sites is exothermic. An Evans-Polanyi plot for reactions of ^3O with alkanes extrapolates to a very low value for the activation energy of H abstraction from toluene of $\approx 10 \text{ kJ/mol}$. Accordingly, H abstraction might be expected to constitute a main channel. In contrast, in a shock tube investigation of reaction (4) the OH channel has been determined to account for only 10% at $T \approx 1100 - 1350 \text{ K}$. In a crossed molecular beam study of reaction (4) the addition-elimination products $\text{CH}_3 + \text{phenoxy}$ and $\text{H} + \text{cresoxy}$ were observed [10b]. Note also that the similarity of reactivities of toluene, ethylbenzene, and cumene despite of the significantly distinct benzylic C-H bond energies can be taken as evidence against H abstraction. However, an unambiguous answer cannot yet be given. Further experimental work is underway [12].

REACTIONS OF $^3\text{CH}_2$ WITH UNSUBSTITUTED AROMATICS: The rate parameters for the corresponding reactions of $^3\text{CH}_2$,

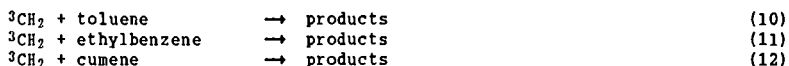


are listed in Table 1 [5b, e]. The different data points obtained from the LMR measurements and, for benzene, from an analysis of stable end products at room temperature are plotted in Arrhenius form in Fig. 1. Corrections for contributions from excitation to the singlet state and consecutive $^1\text{CH}_2$ reactions were applied as described [7]. In comparison to ^3O , $^3\text{CH}_2$ can be seen to be significantly less reactive. In particular, the reaction of $^3\text{CH}_2$ with benzene (7) exhibits almost twice as high an activation energy, its value being virtually equal to the CH_2 singlet-triplet splitting. Reactions (8) and (9) can be seen to be faster than (8), similar to the observations for ^3O , but still slower than $^3\text{O} + \text{benzene}$.

Fig. 3 shows product histograms for $^3\text{CH}_2$ as well as $^1\text{CH}_2 + \text{benzene}$ [5a]. $^3\text{CH}_2$ reacts via addition to the ring system. The product distributions under different conditions, including flame temperatures, can be rationalized with the help of unimolecular rate theory and the energy diagram of Fig. 4. At room temperature and pressures above a few mbars the reaction is in its high pressure limit

and cycloheptatriene is the main product. H abstraction by $^3\text{CH}_2$ from the aromatic ring would have an activation energy far above the singlet-triplet separation and thus cannot play a role in practical systems. The observed small yield of toluene (see Fig. 3) is an unambiguous manifestation of the partial thermal equilibration between $^3\text{CH}_2$ and $^1\text{CH}_2$ taking place even at room temperature. $^1\text{CH}_2$ reacts with benzene either via addition to the aromatic ring, giving cycloheptatriene as primary product, or via insertion into a C-H bond to yield toluene. Reaction products of naphthalene and phenanthrene can be rationalized by analogy.

REACTIONS OF $^3\text{CH}_2$ WITH ALKYL SUBSTITUTED AROMATICS: The results for reactions of $^3\text{CH}_2$ with a series of alkylbenzenes,



are given in Table 1 and illustrated in Fig. 2 [5c, d]. Reaction (11) has been discussed in some detail before [5d]. However, with the data for the related molecules the overall picture becomes apparent. The reactions of $^3\text{CH}_2$ with alkylbenzenes have much higher activation energies than what has been measured for ^3O . A most striking difference is the observation from Fig. 2 that the rate coefficients for (10) - (12) cannot be represented by single Arrhenius expressions. Instead, one has to distinguish two regimes. At high temperatures (> 450 K) the different alkylbenzenes exhibit virtually identical kinetics, regardless of the nature of the side group. "High temperature" activation energies for all three molecules are close to the one for benzene, suggesting addition of the $^3\text{CH}_2$ to the ring to account for the reaction. Similar behaviour has also been observed for p-xylene [5c]. Product yields can be predicted using unimolecular rate theory [5d]. At temperatures below 450 K reaction channels with much lower activation energies and lower preexponential factors play a role, and the kinetics of toluene, ethylbenzene, and cumene become distinct. Measured product distributions (see Fig. 3, [5a]) for reactions (10) and (12) indicate the importance of H abstraction from the alkyl groups of these molecules under these conditions. The observed high yields of ethylbenzene from (10) or n-propylbenzene and cumene from (11) are produced via the subsequent cross recombination of the primary products CH_3 and the respective "benzyl" radicals, e.g.



The combination of addition and abstraction channels produces the apparent curvature in the Arrhenius plots.

DISCUSSION: The general observation has been that $^3\text{CH}_2$ is a much less reactive species than ^3O . However, interesting common trends as well as some differences can be observed which shall be pointed out in the following.

From a study of H abstraction reactions from saturated hydrocarbons [7] the reactivities of $^3\text{CH}_2$ are to vary with reactants in a manner parallel to the better known trends for ^3O . Fig. 5 shows the respective correlation. The differences in the activation energies for both species are of the order of only 5 kJ/mol. However, the bond strength is higher in the product H- CH_2 than in H-O (461 kJ/mol vs. 428 kJ/mol). The preexponential factors for reactions of $^3\text{CH}_2$ had been found to be lower by roughly an order of magnitude than for ^3O , reflecting the steric requirements to form the transition states [7].

The reactions of ^3O and $^3\text{CH}_2$ with the aromatic hydrocarbons, as with other unsaturated reactants, are dominated by the electrophilic character of the radicals.

The correlations between activation energies for corresponding reactions are shown in Fig. 5. Different families of reactants (alkenes vs. alkyne vs. unsubstituted aromatics vs. alkylaromatics) exhibit different trends. For ^3O the activation energies are known to correlate with the ionization potentials of the reactants [13, 3d]. Analogous trends can be observed for $^3\text{CH}_2$. Some theoretical support for such a correlation stems from recent ab initio quantum chemical computations of the potential energy surface for the reaction of $^3\text{CH}_2$ with C_2H_4 by Peyerimhoff and coworkers [14], who found the critical phase of the reaction to be accompanied by a charge transfer from the C_2H_4 moiety towards the methylene C. Loosely speaking, the energetics of the transition state regions might thus be expected to depend on the ease of charge transfer from the reactant, for which the ionization potential is a rough measure. Other factors, however, play a role as well. For instance, the activation energies for reaction of $^3\text{CH}_2$ with tetramethylethylene and cycloheptatriene have been observed to be much higher than expected from the simple correlations [5e]. For the first molecule hindrance by the methyl groups must be considered, whereas for the latter electronic effects due to the three conjugated π -bonds can play a role.

The preexponential factors for the addition reactions of ^3O and $^3\text{CH}_2$ to aromatics differ little. It is noted, however, that the $^3\text{CH}_2$ values depend on the correction for the pathway via excitation of $^3\text{CH}_2$ to the singlet state. Thus, they contain somewhat higher systematic uncertainties than the activation energies. In view of the spectroscopically known singlet-triplet couplings in CH_2 , it is an interesting speculation, whether the chemical differences between " $^1\text{CH}_2$ " and " $^3\text{CH}_2$ " decrease towards high temperatures (high internal excitation). $^1\text{CH}_2$ is known to react with hydrocarbons with close to unit collision efficiency [8]. At room temperature, the observed distinct products of CH_2 in the two spin configurations indicate that both species do react independently. This picture is substantiated by the ab initio potential surface of Peyerimhoff [14], who showed the minimum energy pathways for the approach of CH_2 in both spin states to C_2H_4 to be entirely different, leaving little room for singlet-triplet conversion during the reaction. Instead, CH_2 singlet-triplet intersystem crossing seems to be governed by long-range processes [8, 15]. Little is known, however, about the reaction dynamics of $^3\text{CH}_2$ in vibrationally excited states, which would certainly be of importance under the conditions of combustion processes. In any case, for modeling combustion processes the distinct chemistry of $^1\text{CH}_2$, which has been well established now [8] but which cannot be discussed here in more detail has to be taken into account.

REFERENCES

- [1] (a) K. H. Homann, 20th Symposium (International) on Combustion, p. 857 (1985); (b) B. S. Haynes, H. Gg. Wagner, Prog. Energy Comb. Sci. 7, 229 (1981); (c) I. Glassman, 22nd Symposium (International) on Combustion, p. 295 (1989).
- [2] P. Jensen, P. R. Bunker, J. Chem. Phys. 89, 1327 (1988).
- [3] (a) M. Tappe, V. Schliephake, H. Gg. Wagner, Z. Phys. Chem. NF 162, 129 (1989); (b) H. Frerichs, R. Koch, M. Tappe, H. Gg. Wagner, Z. Naturforsch 44a, 1119 (1989); (c) H. Frerichs, M. Tappe, H. Gg. Wagner, Ber. Bunsenges. Phys. Chem. 94, 1404 (1990); (d) H. Frerichs, M. Tappe, H. Gg. Wagner, 23rd Symposium (International) on Combustion, p. 000 (1990); (e) H. I. Leidreiter, H. Gg. Wagner, Z. Phys. Chem. NF 165, 1 (1989); (f) A. Hoffmann, M. Klatt, H. Gg. Wagner, Z. Phys. Chem. NF 168, 1 (1990); (g) H. Frerichs, R. Koch, V. Schliephake, M. Tappe, H. Gg. Wagner, Z. Phys. Chem. NF 166, 145 (1990); (h) H. Frerichs, V. Schliephake, M. Tappe, H. Gg. Wagner, Z. Phys. Chem. NF 165, 9 (1989); (i) H. Frerichs, M. Tappe, H. Gg. Wagner, Z. Phys. Chem. NF 162, 147 (1989); (j) H. Frerichs, V. Schliephake, M. Tappe, H. Gg. Wagner, Z. Phys. Chem. NF 166, 157 (1990).
- [4] T. Böhland, F. Temps, H. Gg. Wagner, Z. Phys. Chem. NF 142, 129 (1984).

- [5] (a) K. Heberger, MPI f. Strömungsforschung, Report 4a/1988, Göttingen, 1988; (b) T. Böhland, F. Temps, H. Gg. Wagner, Ber. Bunsenges. Phys. Chem. 93, 80 (1989); (c) S. Völker, Diplom Thesis, Göttingen, 1987; (d) K. Heberger, F. Temps, S. Völker, W. Wolf, H. Gg. Wagner, 23rd Symposium (International) on Combustion, p. 000, 1990; (e) H. Kraus, Diplom Thesis, Göttingen, 1991.
- [6] C. C. Hayden, D. M. Neumark, K. Shobatake, R. K. Sparks, Y. T. Lee, J. Chem. Phys. 76, 3607 (1982).
- [7] (a) S. Dobe, T. Böhland, F. Temps, H. Gg. Wagner, Ber. Bunsenges. Phys. Chem. 89, 432 (1985); (b) T. Böhland, S. Dobe, F. Temps, H. Gg. Wagner, Ber. Bunsenges. Phys. Chem. 89, 1110 (1985); T. Böhland, S. Dobe, F. Temps, H. Gg. Wagner, MPI f. Strömungsforschung, report 11/1985, Göttingen, 1985.
- [8] (a) M. N. R. Ashfold, M. A. Fullstone, G. Hancock, G. W. Ketley, Chem. Phys. 55, 245 (1981); (b) A. O. Langford, H. Petek, C. B. Moore, J. Chem. Phys. 78, 6650 (1983); (c) T. Böhland, F. Temps, H. Gg. Wagner, Ber. Bunsenges. Phys. Chem. 89, 1013 (1985); (d) W. Hack, M. Koch, H. Gg. Wagner, A. Wilms, Ber. Bunsenges. Phys. Chem. 92, 674 (1988); (e) W. Hack, M. Koch, R. Wagne-ner, H. Gg. Wagner, Ber. Bunsenges. Phys. Chem. 93, 165 (1989); (f) R. Wagne-ner, Z. Naturforsch. 45a, 649 (1990).
- [9] E. Clar, The Aromatic Sextett, Wiley, 1972.
- [10] (a) S. J. Sibener, R. J. Buss, P. Casavecchia, T. Hirooka, Y. T. Lee, J. Chem. Phys. 72, 4341 (1980); (b) R. J. Baseman, R. J. Buss, P. Casavecchia, Y. T. Lee, J. Am. Chem. Soc. 106, 4108 (1984).
- [11] H. Hippler, J. Troe, J. Phys. Chem. 94, 3803 (1990).
- [12] W. Hack, H. Thiesemann, H. Gg. Wagner, unpublished results.
- [13] R. E. Huie, J. T. Herron, Progr. React. Kinet. 8, 1 (1975).
- [14] W. Reuter, B. Engels, S. D. Peyerimhoff, in press.
- [15] (a) U. Bley, M. Koch, F. Temps, H. Gg. Wagner, Ber. Bunsenges. Phys. Chem. 93, 833 (1989); (b) U. Bley, F. Temps, 19th Informal Conference on Photoche-mistry, Ann Arbor, 1990.

TABLE 1: Arrhenius parameters for reactions of ^3O and $^3\text{CH}_2$ with aromatics.

Reaction	A [$\text{cm}^3/\text{mol}\cdot\text{s}$]	E_a [kJ/mol]
^3O + benzene	$2.4 \cdot 10^{13}$	19.5
^3O + naphtalene	$1.4 \cdot 10^{13}$	7.5
^3O + phenanthrene	$1.9 \cdot 10^{13}$	7.7
^3O + toluene ^{a)}	$2.2 \cdot 10^{13}$	15.6
^3O + ethylbenzene ^{a)}	$2.2 \cdot 10^{13}$	15.9
^3O + cumene ^{a)}	$2.0 \cdot 10^{13}$	15.3
$^3\text{CH}_2$ + benzene	$3.0 \cdot 10^{13}$	37.9
$^3\text{CH}_2$ + naphtalene	$1.3 \cdot 10^{13}$	27.9
$^3\text{CH}_2$ + phenanthrene	$2.2 \cdot 10^{13}$	28.3
$^3\text{CH}_2$ + toluene ^{b)}	$6.0 \cdot 10^{13}$	36.8
$^3\text{CH}_2$ + toluene ^{c)}	$2.0 \cdot 10^{11}$	19.0
$^3\text{CH}_2$ + ethylbenzene ^{b)}	$6.0 \cdot 10^{13}$	36.8
$^3\text{CH}_2$ + ethylbenzene ^{c)}	$1.6 \cdot 10^{11}$	13.6
$^3\text{CH}_2$ + cumene ^{b)}	$6.0 \cdot 10^{13}$	36.8
$^3\text{CH}_2$ + cumene ^{c)}	$3.0 \cdot 10^{11}$	13.6

a) Presumably addition reaction, see text.

b) Addition reaction to aromatic ring, see text.

c) Estimated values, H atom abstraction from alkyl group, see text.

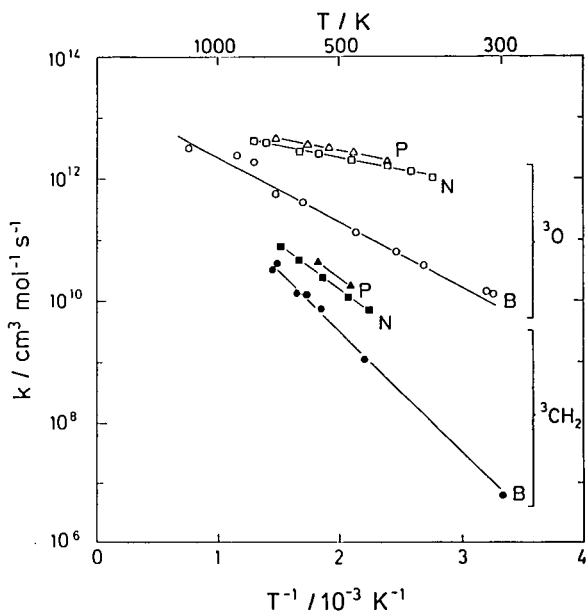


FIGURE 1: Arrhenius plot for the reactions of ^3O and $^3\text{CH}_2$ with benzene (B), naphthalene (N), and phenanthrene (P).

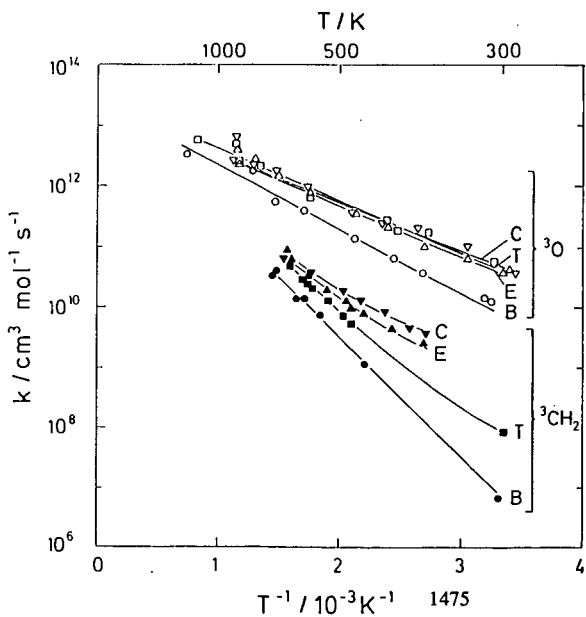


FIGURE 2: Arrhenius plot for the reactions of ^3O and $^3\text{CH}_2$ with benzene (B), toluene (T), ethylbenzene (E), and cumene (C).

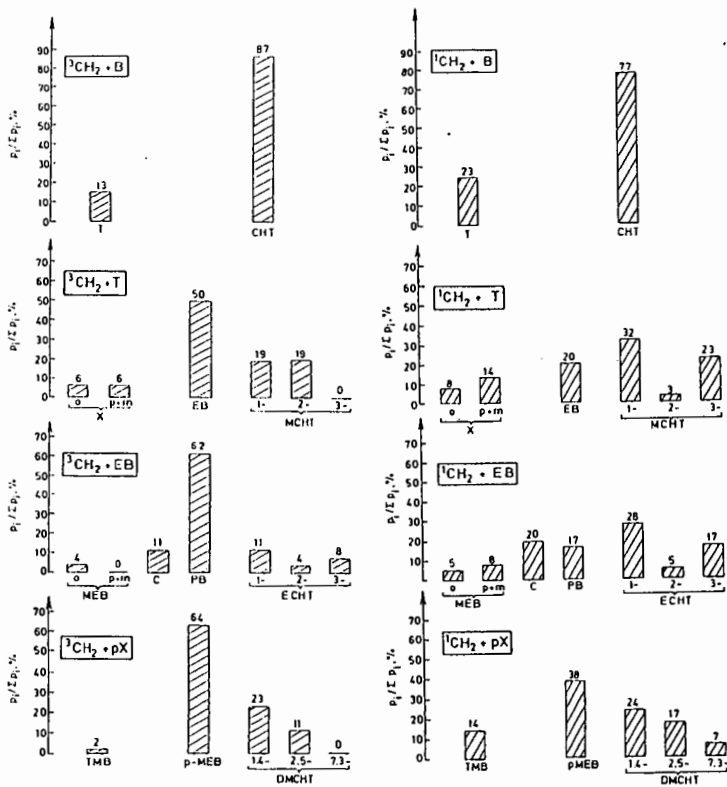


FIGURE 3: End product distributions for the reactions of $^3\text{CH}_2$ and $^1\text{CH}_2$ with benzene, toluene, ethylbenzene, and p-xylene [5a]. B = benzene, T = toluene, CHT = cycloheptatriene, X = xylene, EB = ethylbenzene, MCHT = methylcycloheptatriene, MEB = methylethylbenzene, C = cumene, PB = n-propylbenzene, ECHT = ethylcycloheptatriene, TMB = trimethylbenzene, MEB = methylethylbenzene, DMCHT = dimethylcycloheptatriene.

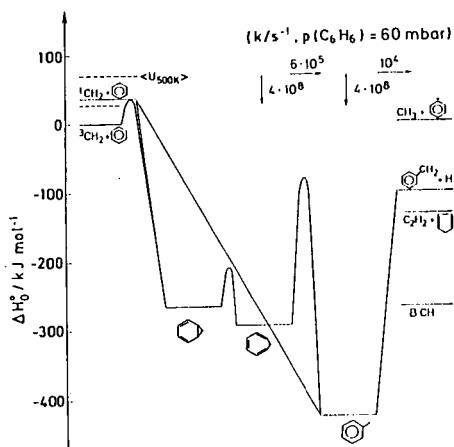


FIGURE 4: Energy diagram for the reactions of ³CH₂ and ¹CH₂ with benzene [5b].

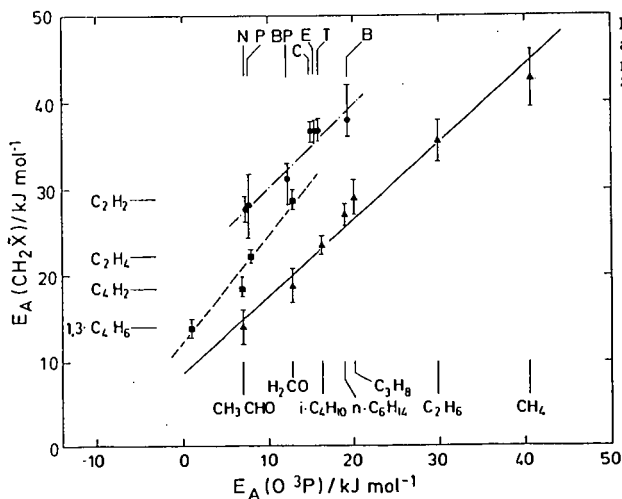


FIGURE 5: Correlation of activation energies for reactions of ³O and ³CH₂.

BENZENE/TOLUENE OXIDATION MODELS: STUDIES BASED ON FLOW-REACTOR AND
LAMINAR FLAME SPEED DATA

K. Brezinsky, F.N. Egolfopoulos, J.L. Emdee, C.K. Law and I. Glassman
Department of Mechanical and Aerospace Engineering
Princeton University
Princeton, N.J. 08544

Introduction

Aromatic hydrocarbons are expected to remain significant components of gasolines and jet fuels because they offer many advantages such as a high energy density (Goodger and Vere, 1985) and a high knock rating (ASTM Special Technical Publication No. 225, 1958). In working towards a comprehensive understanding of aromatic combustion, the high temperature oxidation mechanism of toluene has been studied extensively at Princeton (Euchner, 1980, Venkat et al., 1983, Brezinsky et al., 1984, Brezinsky, 1986, Litzinger, 1986, Brezinsky et al., 1990). The mechanistic details that evolved in those studies have indicated that at temperatures near 1000 K and 1 atmosphere pressure the early time oxidation characteristics are dominated by side chain chemistry followed by aromatics ring attack. The reactions of the small molecule fragments of the aromatic ring, for the most part, occur later in the reaction sequence; therefore a modest sized model, based largely on the mechanisms given by Brezinsky (1986) for the oxidation of toluene near 1200 K. This model captures the early time chemistry and the essential details of the later time small molecule reactions for both toluene and benzene at flow reactor conditions. The success of this model in predicting flow reactor species profiles, as will be briefly described in the succeeding paragraphs, led to the application of the model to the calculation of laminar flame speeds. The results of these calculations will be described.

Experimental Data for Model Verification

The toluene oxidation data of Brezinsky et al. (1984) and the benzene oxidation data of Lovell et al. (1989) were used to verify the toluene model and its benzene sub-mechanism. These data were from Princeton flow reactor experiments and include lean and rich equivalence ratios (ϕ) with initial temperatures from 1100 K to 1190 K. The experimental details are described in the individual papers.

Slight adjustments were made to the data presented in the above two references to reflect recent calibration of the flow reactor rotameters and velocity profile. The effect of these recent changes is to give reaction times which are approximately 15-20% shorter than given in the original papers. It should be noted that the velocity profile in the reactor tube is still under investigation. Further details regarding the reduction of the experimental data can be found in Emdee (1991).

Description and Analysis of the Model

The model consists of 68 reactions forming a benzene sub-model and 62 additional reactions for the toluene model. A complete description of the model and associated thermodynamic properties of the chemical species is available (Emdee et al., 1991; Emdee, 1991). Since benzene is a key intermediate in the oxidation of toluene, the benzene sub-model results will be considered before the toluene model is discussed.

Comparison of the Benzene Oxidation Model and Experimental Data

The flow reactor experiments approximate an adiabatic, constant

pressure, reaction system in which hydrodynamic and diffusional transport effects are small compared to changes brought about by chemical reaction. Thus, to make a comparison between the experimental data and the kinetic model, the reaction system was numerically treated as a time-dependent, adiabatic, constant pressure, homogenous mixture using CHEMKIN (Kee et al., 1980). Since mixing of the fuel and oxygen in the diffuser section of the flow reactor shortens the time for initial consumption of the fuel, the experimentally derived reaction time is only relative. Thus the comparison between experiment and model was made after shifting the experimental data in time so that the experimental fuel concentration at 50% of the measured consumption matched the model prediction. The time shift was constant for each experimental condition.

The experimental data and model results for benzene are compared in Fig. 1. Intermediate species profiles are shown for the $\phi = 0.91$ case only; further results for other conditions can be found in Emdee (1991).

The model prediction of the fuel decay was in good agreement with the experimental data for all three conditions considered. A fair match was achieved between the total C_4 and C_2 species. Lovell et al., did not make a distinction between the C_4 's and the C_2 's. However, they did indicate that the C_4 's were vinyl acetylene (C_4H_4) and butadiene (C_4H_6) in about a 3:1 ratio, and the C_2 's were "predominately acetylene and some ethylene". Because the present model can distinguish between species, the individual components of the C_4 's and C_2 's are also plotted in Fig. 1. The vinyl acetylene to butadiene ratio appears similar to the ratio indicated by Lovell et al., and the acetylene mole fraction is much larger than the ethylene mole fraction.

The mole fractions of phenoxy and cyclopentadienyl are included in the comparisons of phenol and cyclopentadiene because these species are resonantly stable and might be expected to build up to relatively high concentrations. If these radical species found a source of H in the sampling probe, they would have been detected as the stable parent species. Figure 1 shows that the inclusion of these radicals in the total phenol and cyclopentadiene profiles has a small effect on the former and a large effect on the latter.

Although good agreement between the predicted and experimental phenol profiles was achieved for the lean and near stoichiometric conditions, the model tended to underpredict the phenol mole fractions for rich conditions. The cyclopentadiene profiles were predicted with fair agreement by the total of the C_8H_8 and C_5H_6 concentrations for the lean and near stoichiometric conditions but was overpredicted by the rich condition. The overprediction of the cyclopentadiene coupled with the underprediction of the phenol for the rich case suggests that phenol is being consumed too quickly for this case. Carbon monoxide was underpredicted for all equivalence ratios considered which in part reflects the lack of a full sub-mechanism for small molecule chemistry.

Comparison of the Toluene Oxidation Model and the Experimental Data

The results of the calculations are shown in Figs. 2. The toluene model did very well at predicting the fuel consumption rate as well as the concentrations of many of the aromatic intermediates including benzene, benzaldehyde, ethylbenzene, benzyl alcohol and styrene for both lean and rich conditions. The concentrations of both phenol and cresol were however always underpredicted.

The figures show that the amounts of acetylene suggested by the model are at least a factor of two larger than the experimentally measured values.

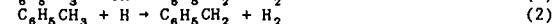
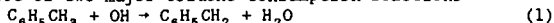
All of the acetylene comes from the C_4 species which, although not shown, were underpredicted by the toluene model. Thus even though the C_2 's and C_4 's were predicted with fair agreement for the oxidation of benzene near 1100 K, the higher temperature (≈ 1190 K) oxidation model of toluene suggests that the decomposition rate of the C_4 's to the C_2 's may not have the correct temperature dependence.

In contrast to the benzene oxidation model in which CO was underpredicted, the CO concentrations predicted by the toluene model matched well with the experimental data. The better CO prediction by the toluene model can be partially attributed to the greater understanding of side chain chemistry which dominates the early oxidation of toluene as compared to the limited understanding of ring chemistry which was important in the oxidation of benzene.

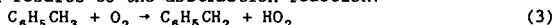
Summary of Flow Reactor Modeling

By constructing a kinetic model for the oxidation of toluene based on mechanistic and kinetic information from the literature and from thermochemical estimates, it was possible to reasonably model flow reactor oxidation experiments of benzene and toluene. The consumption rate of toluene and benzene for both lean and rich oxidation conditions is predicted quite well by the model as are many of the intermediates. The predictive capability of the model is a significant improvement over previously reported results (Bittker, 1987, 1988, 1991; Fujii and Asaba, 1973; McLain et al., 1979).

The inhibitory effect of two major toluene consumption reactions



was clearly indicated by a linear sensitivity analysis. Furthermore, the high sensitivity of the model results to the abstraction reaction:



has allowed for an estimate of this reaction rate constant with reasonable confidence.

The major shortcomings of the model were found to be the over prediction of acetylene and the under-prediction of phenol compounds. The acetylene profiles were not predicted correctly for the higher temperature toluene oxidation even though the lower temperature benzene sub-model predicted reasonable levels. With regard to the phenol formation, the temperature dependence of the decomposition rate of phenoxy was expected to be the source of error since phenol was predicted reasonably well in the lower temperature benzene sub-model.

Flame Modelling

The modelling of measured laminar flame speeds, S_{L1} , over a range of temperatures and pressures has been demonstrated to be an effective technique for developing and refining comprehensive chemical kinetic models (Egolfopoulos et al., 1991). For such modelling purposes, limited data from the measurement of laminar flame speeds of toluene and/or benzene are available in the literature (Garner et al., 1951, Gerstein et al., 1951, Wagner and Dugger, 1955, and Gibbs and Calcote, 1959). The encyclopedic work of Gibbs and Calcote (1959) contains flame speeds for benzene at atmospheric pressure over an equivalence ratio of 0.8 - 1.3. These values were obtained using a bunsen burner conical flame and shadowgraphs for definition of the flame surface. Fristrom and Westenberg (1965) have pointed out the complications in defining the flame surface by shadowgraphy and these complications would affect the magnitude of the flame velocities reported by

Gibbs and Calcote. Similarly, Law (1988) has emphasized the role that flame stretch can play in the determination of flame speeds and pointed out the substantial variation in measured values that can result if the flame speeds are not evaluated in the limit of zero stretch (Egolfopoulos et al. 1989). All the aromatics flame speeds reported in the literature are affected by stretch. In the absence of stretch free flame speeds for aromatics, the flame speed values for benzene measured by Gibbs and Calcote were used for comparison with model predictions since their measurement technique tended to minimize stretch effects:

ϕ =	.8	.9	1.0	1.1	1.2	1.3
S_u =	39.4	45.6	47.6	44.8	40.2	35.6 (cm/sec)

The data on the flame speeds of toluene are much more limited than for benzene. The value commonly found in textbooks for a stoichiometric, one atmosphere flame, 38.8 cm/sec, is attributable to Wagner and Dugger (1955). For comparison with the Gibbs and Calcote measured value, the stoichiometric, one atmosphere benzene flame speed measured by Wagner and Dugger was 44.6 cm/sec.

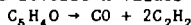
In order to model the reported flame speeds, the toluene model derived from flow reactor experiments was coupled to the PREMIX code (Kee et al., 1985). The calculated flame speeds for stoichiometric toluene/air and benzene/air mixtures were approximately 23 cm/sec - a value far beyond the range of error of the measured values. The low calculated flame speeds implied that the aromatics combustion process was not proceeding fast enough to the energy releasing, small molecule oxidation steps. The toluene model contained only a very basic sub-mechanism for the oxidation of species containing two or less carbon atoms in order to keep the number of reactions and species small. Therefore, the first attempt at altering the mechanism to obtain a higher flame speed consisted of replacing the abbreviated C_2 oxidation scheme with a more complete, validated one (Egolfopoulos et al., 1991). The substitution of this C_2 scheme led to a marginal increase of only 4 cm/sec.

A sensitivity analysis of the flame speed to each rate constant in the toluene model indicated that there was little sensitivity (less than 2%) to the alkyl side chain oxidation steps. Greater sensitivity (2% or more) was found for a subset of nine rate constants directly related to the oxidation of the aromatic ring and its fragments. The benzene flame calculations revealed a sensitivity to these same reactions. Of course, the greatest sensitivity of the flame speed was found to be for the $CO + OH \rightarrow CO_2 + H$ reaction (11%) and for $H + O_2 \rightarrow OH + H$ (21%). Since these latter two reactions have been extensively studied no further consideration was given to changing their rate constants. In view of the greater availability of benzene flame speed data and the sensitivity of both the toluene and benzene flame speeds to the same rate constants, the toluene mechanism was reduced, for ease of calculation and analysis, to a benzene mechanism by the removal of all the toluene related steps.

Among the rate constants having the most effect on the flame speed a number are uncertain either because they are estimated rather than measured, measured over a narrow range of temperature, or have been determined in only one set of experiments. Therefore, sequentially for each uncertain rate constant, the value of A in the three parameter representation of the rate constant, $k = AT^n \exp(E_a/RT)$, was increased or decreased as indicated by the sensitivity analysis in order to "walk" the flame speed up into the 40 cm/sec range:

$C_6H_5O + H \rightarrow C_6H_5OH$; forward A decreased by 2.5 x; reverse increased 10x
 $C_6H_5O \rightarrow C_6H_5 + CO$; forward A increased 10x
 $C_6H_5 + O_2 \rightarrow C_6H_5O + O$; forward A increased 10x
 $C_6H_5 + OH \rightarrow C_6H_5OH + H$; forward A increased 10x

The result of the above changes was a calculated flame speed of 41.6 cm/sec. A sensitivity analysis of this calculated flame speed indicated that changes in the rate constants of the three reactions of C_6H_5 species would have a significant effect (2% or more) on the flame speed. A ten fold increase in the forward and reverse A values of



was sufficient to raise the stoichiometric flame speed to 43.8 cm/sec, a value lower than that measured by Gibbs and Calcote but within the range seemingly appropriate for benzene. The calculated flame speeds at other equivalence ratios were 31.2, 38.2, 48.7, and 50.1 cm/sec at $\phi = 0.8, 0.9, 1.1$ and 1.2 respectively.

Species profiles calculated with the altered model for flow reactor conditions were significantly changed from those described earlier in this article. The changes were not surprising since the altered rate constants were the same ones shown by sensitivity analysis of the benzene decay profile to be significant during the flow reactor modelling efforts. In particular, the altered rate constants led to an order of magnitude decrease in initial benzene concentration within 60 msec, maximization of the phenol concentration within 30 msec and, CO production and almost complete consumption within 120 msec. These latter observations suggest how the toluene/benzene model might be made more comprehensive in order to predict both flow reactor and flame speed results.

The altered model in its ability to approximately match the measured benzene flame speeds has required a much more rapid production and oxidation of the energy releasing, small molecule hydrocarbon fragments. However, the flow reactor profiles indicate that alteration of the rate constants in the above extent and manner is not fully justified. It appears that a subset of toluene/benzene reactions is needed that would not drastically affect the calculated species profiles at flow reactor temperatures but would lead to an accelerated production of small hydrocarbons at flame temperatures. This conclusion has two implications; the temperature dependent parameters of the above mentioned altered rate constants reactions may require re-adjustment in a way already suggested by some of the inadequacies revealed during flow reactor modelling and, the addition of high activation energy pyrolysis reactions, such as aromatic ring rupture steps, not currently in the toluene/benzene mechanism may be necessary in order to provide H atoms to drive the overall reaction progress. Both of these approaches to creating a comprehensive toluene/benzene model are currently being pursued.

Acknowledgement: The support of this research by the Department of Energy, Office of Basic Energy Sciences, through Grant DE-FG02.86ER3554 is gratefully acknowledged.

References

- ASTM Special Technical Publication No. 225; American Society of Testing Materials, Philadelphia, 1958.
- Bittker, D. A., Detailed Mechanism of Benzene Oxidation; NASA Tech. Memo. 100202, 1987.
- Bittker, D. A., Detailed Mechanism of Toluene Oxidation and Comparison with Benzene; NASA Tech. Memo. 100261, 1988.
- Bittker, D. A., *Combust. Sci. Technol.* 1991, in press.
- Brezinsky, K., Litzinger, T. A. and Glassman, I., *Int. J. Chem. Kinet.* 1984, 16, 1053.
- Brezinsky, K., *Prog. Energy Combust. Sci.* 1986, 12, 1.
- Brezinsky, K., Lovell, A. B. and Glassman, I., *Combust. Sci. Technol.* 1990, 70:1-3, 33.
- Egolfopoulos, F.N., Cho, P. and Law, C.K., *Combust. Flame* 1989, 76, 375.
- Egolfopoulos, F.N., Du, D.X. and Law, C.K., *Combust. Sci. Technol.* 1991, submitted.
- Emdee, J. L., An Experimental and Modeling Study of the High Temperature Oxidation of the Xylenes; Ph.D. Thesis, Department of Mechanical and Aerospace Engineering, Princeton University, Princeton, NJ, 1991.
- Emdee, J. L., Brezinsky K. and Glassman, I., *J. Phys. Chem.* 1991, submitted.
- Euchner, J. A.: M.S.E. Thesis, Department of Mechanical and Aerospace Engineering, Princeton University, Princeton, NJ, 1980.
- Fristrom, R.M. and Westenberg, A.A., *Flame Structure*, 1965, McGraw-Hill.
- Fujii, N. and Asaba, T., *Fourteenth Symp. (Int.) Combust.*; The Combustion Institute, Pittsburgh, 1973, p.433.
- Garner, F.H., Long, R. and Ashforth, G.K., *Fuel* 1951, 30, 17.
- Gibbs, G.J. and Calcote, H.F., *J. Chem. Eng. Data*, 1959, 4, 226.
- Goodger, E. and Vere, R., *Aviation Fuels Technology*; MacMillan Publishers Ltd., London, 1985.
- Kee, R. J., Miller, J. A. and Jefferson, T. H., CHEMKIN: A General Purpose, Problem-Independent, Transportable, Fortran Chemical Kinetics Code Package; Sandia Nat. Lab. Report SAND80-8003, 1980.
- Kee, R. J., Grcar, J. F., Smooke, M. D., and Miller, J. A. PREMIX; A Fortran Program for Modeling Steady Laminar One-Dimensional Premixed Flames; Sandia Report SAND 85-8240 UC4, 1985.
- Kee, R. J., Rupley, F. M., and Miller, J. A. The Chemkin Thermodynamic Data Base; Sandia Nat. Lab. Report SAND87-8215, 1987.
- Law, C.K., *Twenty-Second Symp. (Int.) Combust.*; The Combustion Institute, Pittsburgh, 1988, 1381.
- Litzinger, T. A.: Ph.D. Thesis, Department of Mechanical and Aerospace Engineering, Princeton University, Princeton, NJ, 1986.
- Litzinger, T. A., Brezinsky, K. and Glassman, I., *Combust. Flame* 1986, 63, 251.
- Lovell, A. B., Brezinsky, K. and Glassman, I., *Twenty-Second Symp. (Int.) Combust.*; The Combustion Institute, Pittsburgh, 1989, p.1063.
- McLain, A. G., Jachimowski, C. J. and Wilson, C. H., Chemical Kinetic Modeling of Benzene and Toluene Behind Shock Waves; NASA Tech. Paper 1472, 1979.
- Wagner, P. and Dugger, G.L., *J. Am. Chem. Soc.* 1955, 77, 227.
- Venkat, C., Brezinsky, K., and Glassman, I., *Nineteenth Symp. (Int.) Combust.*; The Combustion Institute, Pittsburgh, 1983, p.143.

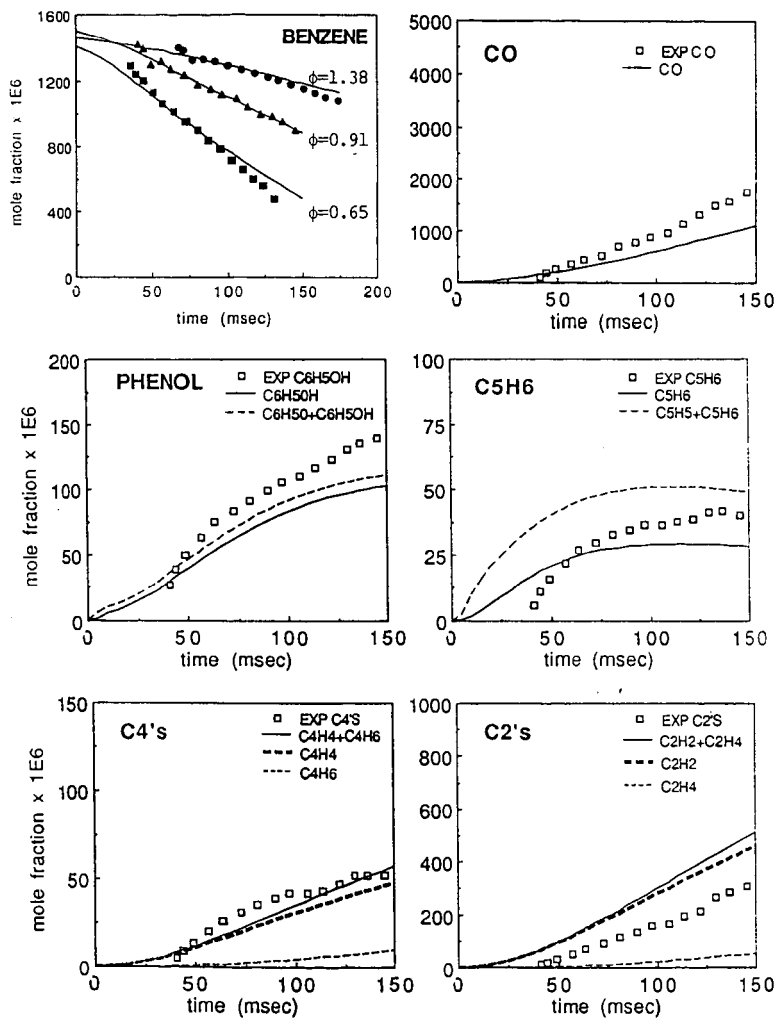


Fig. 1. Experimental (symbols) and model (lines) benzene decay profiles for three different equivalence ratios and intermediates experimental and model profiles for a $\phi=0.91$ oxidation of benzene.

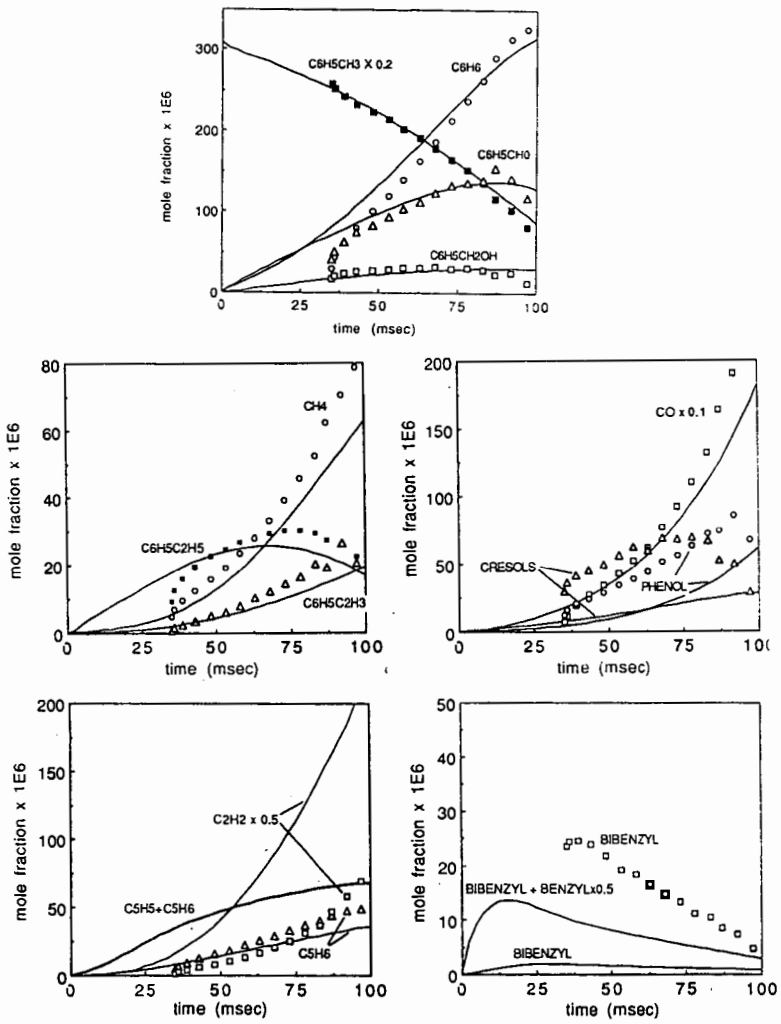


Fig. 2. Experimental (symbols) and model (lines) species profiles for a $\phi=0.69$ oxidation of toluene.

A TENTATIVE DETAILED CHEMICAL SCHEME FOR THE OXIDATION OF BENZENE-AIR MIXTURES

Christophe Chevalier, Jürgen Warnatz
Institut für Technische Verbrennung, Universität Stuttgart
Pfaffenwaldring 12, 7000 Stuttgart 80, Germany

Keywords: Kinetics, numerical simulation, laminar flames and ignition of benzene.

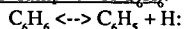
INTRODUCTION

The increasing use of unleaded gasoline in western countries in the last 20 years has forced oil companies to find substitutes for the alkyl-lead compounds, in order to supply high-octane fuels. Among aromatic hydrocarbons, which are well known to have a high octane number, benzene is a preferred compound (up to 5% or more in liquid commercial fuels). Unfortunately, it has a pronounced propensity to form soot during its combustion (1). Nevertheless, a rather limited number of works on detailed chemical schemes has been published yet. Early studies considered the low temperature ignition of aromatic hydrocarbons in static reactors (2-9), where a major step is the addition of molecular oxygen to a phenyl radical, leading to a bridging peroxy radical which, according to Benson (10), is very unlikely to be formed at temperatures above 700 K. More recently shock tube (11) and flow reactor (12-15) experiments have pointed out the most important pathways at higher temperatures. It appears that a phenyl radical and O_2 react to form a phenoxy radical and an O atom. However, no detailed reaction mechanism for the oxidation of benzene in flames and for its auto-ignition over a wide range of conditions has been published yet. Based on a review of the rate coefficients proposed for each elementary reaction, a detailed chemical scheme is presented and discussed here. Numerical simulations of premixed laminar flames, and calculations of auto-ignition delay times are compared with experiments, in order to check the validity of the mechanism.

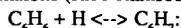
REACTION MECHANISM

The reaction mechanism presented here is based on a high temperature gas phase mechanism, which has been developed recently (16) for saturated and unsaturated hydrocarbons up to C_4 . However, due to lack of space, this work (including several hundreds of literature references) cannot be presented here. Most of rate coefficients of the reactions involving C_6H_6 follow the recommendations of the CEC evaluation group (17). The reverse reaction rates have been calculated using the equilibrium constants (reactions characterized by " \leftrightarrow "). Irreversible steps are denoted by " \rightarrow ". Reactions directly related to the oxidation of benzene are discussed here, and summarized in table 1. The complete detailed mechanism contains 57 species and 475 elementary reactions.

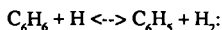
1) Consumption of C_6H_6 :



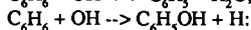
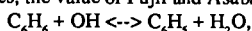
Due to the size of the benzene molecule, a fall-off behavior appears only for very low pressures; thus, at 1 bar, the high pressure rate coefficient may be used (18). This has been confirmed by RRKM calculations (Rice-Ramsberger-Kassel-Marcus theory).



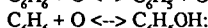
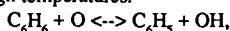
Measurements for this recombination reaction have only been carried out at low temperatures ($T < 1000$ K). The C_6H_7 radical may be one of the possible starting points for an opening of the cycle, but no rate coefficient is available for this step.



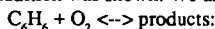
Due to the scatter in the experimental data at high temperatures, it is difficult to evaluate the rate coefficient. Since this abstraction channel is necessary for a mechanism describing combustion in flames, the value of Fujii and Asaba has been taken (19).



At high temperatures, the H-abstraction seems to be the dominant channel. The displacement reaction is probably not an elementary process (proceeding via a $\text{C}_6\text{H}_6\text{OH}$ species), but cannot be neglected at high temperatures.



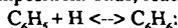
Experiments have been carried out up to 1000 K. Moreover, no clear separation between abstraction and addition was shown. We assumed the same reaction rate for both channels.



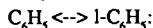
No data was found for this reaction, which may play an important role for the ignition.

2) Consumption of C_6H_5 :

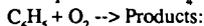
Most of the reactions concerning the phenyl radical have been studied in relation with the thermal decomposition. Thus, reactions with other radicals are not well known.



The reverse of this recombination reaction has been discussed above.

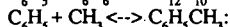
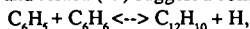


According to Braun-Unkoff et al. (20), who monitored H atoms, the opening of the cycle is the only possible decomposition, the pathways leading to $\text{C}_4\text{H}_3 + \text{C}_2\text{H}_2$, $\text{C}_6\text{H}_4 + \text{H}$, $\text{C}_4\text{H}_2 + \text{C}_2\text{H}_3$, or $\text{C}_4\text{H}_4 + \text{C}_2\text{H}$ either have a too high reaction enthalpy, or produce not enough H atoms. The linear $1\text{-C}_6\text{H}_5$ radical may then decompose either to $\text{C}_4\text{H}_3 + \text{C}_2\text{H}_2$ or to $1\text{-C}_6\text{H}_4 + \text{H}$, both reactions being pressure dependent.



This major oxidation step is unfortunately not well known. Venkat et al. (13) propose the formation of a phenoxy radical $\text{C}_6\text{H}_5\text{O} + \text{O}$, but no rate coefficient for this reaction has been measured.

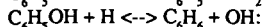
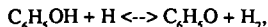
Fujii and Asaba (19) suggest a complex reaction, leading to $\text{C}_6\text{H}_4 + \text{H} + 2\text{CO}$.



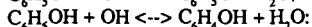
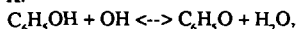
These reactions are not included in the mechanism at the moment, since they lead to biphenyl or toluene, which oxidation would require a much more complex mechanism.

3) Consumption of $\text{C}_6\text{H}_5\text{OH}$:

Phenol is formed in rather high amounts from benzene, by reaction with O and OH (see above), and its oxidation has to be included in the mechanism.



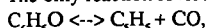
The only experiments available (21) show that the H-abstraction as well as the displacement reaction (the reverse one has been discussed earlier) both are possible at temperatures between 1000 and 1150 K.



This reaction has also been investigated by He and others (21), who do not supply information about the branching ratios.

4) Consumption of C_6H_5O :

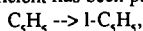
The only reaction reviewed by the CEC (17) has been proposed by Lin and Lin (22):



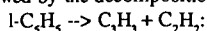
where the decomposition of the phenoxy leads to the formation of a cyclopentadienyl radical.

5) Consumption of C_3H_3 :

This species certainly reacts with radicals like O or OH, as suggested by Brezinsky (14), or with molecular oxygen (Venkat et al. (13)). However, the only pathway involving C_3H_3 for which a rate coefficient has been proposed (20) is reaction



followed by the decomposition



It seems that the lack of radical-radical routes for C_3H_3 is compensated by the semi-global reaction $C_6H_5 + O_2 \rightarrow C_4H_4 + H + 2CO$, since the more detailed scheme proposed by Venkat (13) might be summarized as: $C_6H_5 + O_2 \rightarrow C_6H_5O + O \rightarrow C_3H_3 + CO + O \rightarrow C_3H_3O + CO \rightarrow C_4H_4 + H + 2CO$.

RESULTS AND DISCUSSION

In order to check the mechanism, velocities of freely propagating premixed laminar flames as well as ignition delay times have been calculated, and compared with experiments, under non-sooting conditions (below the sooting limit: $\phi = 1.9$).

1) Laminar flames:

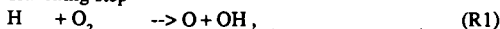
The solid line in Fig. 1 shows the burning velocities of benzene-air mixtures at 298 K and 1 bar, computed for benzene contents from 1.9% to 3.8% (equivalence ratios $\phi = 0.7$ to 1.4). The figure also shows experimental data (23) available for comparison. The maximum computed burning velocity (47.6 cm/s) occurs in stoichiometric mixtures, in agreement with experimental results. For rich mixtures, the computed values lie slightly above the measurements, but in view of the uncertainties in the experiments and in the kinetic data (see above), this difference cannot be considered being significant.

Fig. 2 shows the burning velocities of mixtures containing 1.5% to 5.0% benzene and 20.8% oxygen, diluted with nitrogen (equivalence ratios $\phi = 0.54$ to 1.80), $P = 1$ bar, $T_u = 298$ K, compared with experiments run under the same conditions (24). The maximum calculated speed (49.2 cm/s) is somewhat larger than the measured one (45.0 cm/s), and slightly shifted to lean mixtures ($\phi = 1.1$ instead of $\phi = 1.2$). Around stoichiometry, the computed velocities are found to be too fast (up to 9% discrepancy), but in rich mixtures, they are too slow (40% at most). Since the conditions of this experiment are very similar to those of the one presented first, this result is probably due to the reliability of the measuring techniques.

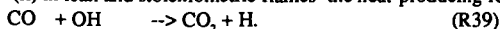
The pathways of the oxidation of C_6H_6 in a stoichiometric benzene/air flame and their relative importance are shown in Fig. 3. C_6H_6 is initially attacked by H, OH, and O radicals to form (i) benzyl radicals, which react with molecular oxygen as described above, (ii) phenol, which, after H-abstraction, leads to cyclopentadienyl radicals. Thus, it is clear that the mechanism leads to two parallel pathways, one being the phenyl route, the other the phenol route.

The sensitivity analysis in Fig. 4 shows the rate limiting reactions, for lean, stoichiometric, and rich mixtures. The sensitivities are obtained by a systematic variation of the preexponential factors of the rate constants. For the i^{th} reaction, the relative sensitivity $S_i = \Delta \ln v_u / \Delta \ln k_i$ denotes the change of the burning velocity with respect to a change of the preexponential factor.

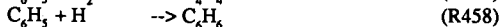
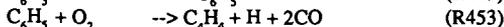
The sensitivity analysis for the reactions of the H_2 -CO- O_2 have been discussed earlier (25, 26). However, it is worth noting that the most sensitive reactions are (i) for all equivalence ratios the chain branching step



(ii) in lean and stoichiometric flames the heat-producing reaction



The reactions which are specific to the combustion of benzene are:



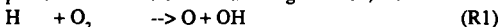
The decomposition of the linear 1- C_6H_5 radical (produced in reaction R449) leads rapidly to the formation of H atoms; therefore, reaction R449 has a positive sensitivity in rich flames, where the molecular oxygen concentration is too low to oxidize all of the phenyl radicals through reaction R453. Reaction R453 directly produces H radicals, and has almost the same sensitivity under lean and under rich conditions. The recombination reaction R458 deprives reaction R1 of H atoms and reactions R449 and R453 of phenyl radicals; its sensitivity is strongly negative. In lean flames, the branching reaction R466 shows a positive sensitivity. The H-consuming reaction R472 has a negative sensitivity, because it competes with reaction R1.

These results point out that a deep insight into the reaction between phenyl and molecular oxygen is fundamental, because the whole mechanism depends on the route chosen.

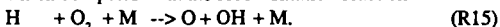
2) Ignition delay times:

Zero-dimensional simulations can be used to calculate ignition delay times of benzene-oxygen-argon mixtures in shock tubes. Fig. 5 shows calculated ignition delay times compared with experimental results of Burcat et al. (27), for stoichiometric mixtures containing 1.69% benzene, at pressures behind reflected shock between 2 and 3 bar, and at temperatures in the range 1286 to 1608 K. If a rather good agreement is observed at the highest temperatures (above 1450 K), an increasing discrepancy appears when decreasing the temperature.

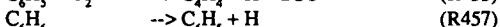
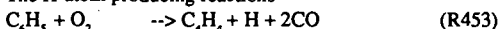
Sensitivity tests with respect to the OH concentration (Fig. 6) show the rate limiting reactions during the induction period at the lowest investigated temperature (1286 K). The main rate-limiting process here is the chain branching reaction, too.



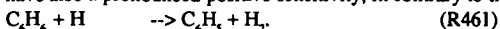
which competes with the recombination reaction



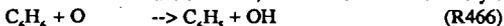
The H-atom producing reactions



have also a pronounced positive sensitivity, in contrary to the H-consuming reaction



Furthermore, the chain branching reaction R466 has a very high positive sensitivity and competes with the termination reaction R468, which has of course a very strongly negative sensitivity:

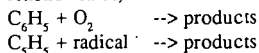


Further information about the relative importance of each channel is necessary to simulate correctly the ignition of benzene-oxygen mixtures.

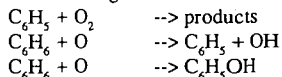
CONCLUSIONS

1- A review of the elementary reactions for the high temperature oxidation of benzene has been carried out, in order to evaluate the current kinetic and thermodynamic knowledge in this field.

2- The calculation of premixed laminar flame velocities of benzene-air mixtures is in good agreement with experiments run at atmospheric pressure, over a wide range of equivalence ratios below the sooting limit. However, it would be helpful to get further data for some reactions (e.g. products, reaction rates):



3- The computed ignition delay times of stoichiometric benzene-oxygen mixtures diluted in argon were 1.5 to 5 times too short compared with shock tube experiments, depending on the temperature. According to sensitivity analyses, these results could certainly be improved by a better knowledge of the following reactions:



4- Based on these results, our preliminary mechanism will be improved in the near future. Calculated and measured species profiles in low pressure laminar flames will be compared, in order to obtain further information about the combustion processes in flames. Furthermore, ignition delay times at pressure ranging from 2 to 7 bar, in lean to rich mixtures will be computed in order to check the mechanism for auto-ignition.

ACKNOWLEDGEMENT

The authors are grateful to Dr. M. Braun-Unkoff and Dr. P. Frank for their interest and helpful discussions.

This research is financed by the commission of the European Communities within the frame of the Joule program, by the Swedish National Board for Technical Development, and by the Joint Research Committee of European automobile manufacturers (Fiat, Peugeot SA, Renault, Volkswagen, and Volvo) within the IDEA program.

REFERENCES

- (1) J.J. MacFarlane, F.H. Holderness, F.S.E. Witcher: *Comb. & Flame* 8, 215 (1964).
- (2) R. Fort, C.N. Hinshelwood: *Proc. Roy. Soc.*, A127, 218 (1930).
- (3) D.W. Newitt, J.H. Burgoyne: *Proc. Roy. Soc.*, A153, 448(1936).
- (4) J.H. Burgoyne: *Proc. Roy. Soc.*, A161, 48 (1937).
- (5) J.H. Burgoyne: *Proc. Roy. Soc.*, A171, 421 (1939).
- (6) J.H. Burgoyne: T.L. Tang, C.M. Newitt, *Proc. Roy. Soc.*, A174, 379 (1940).
- (7) J.H. Burgoyne: *Proc. Roy. Soc.*, A174, 395 (1940).
- (8) J.H. Burgoyne: *Proc. Roy. Soc.*, A175, 539 (1940).
- (9) R.G.W. Norrish, G.W. Taylor: *Proc. Roy. Soc.*, A234, 160 (1956).
- (10) S.W. Benson: *JACS* 87, 972 (1965).
- (11) C.R. Orr: 9th Symp. (Int.) Comb., 1034 (1963).
- (12) R.J. Santoro, I. Glassman: *Comb. Sci. Tech.* 19, 161 (1979).

- (13) C. Venkat, K. Brezinsky, I. Glassman: 19th Symp. (Int.) Comb., 143 (1982).
 (14) K. Brezinsky: Prog. Energy Combust. Sci., 12, 1 (1986).
 (15) A.B. Lovell, K. Brezinsky, I. Glassman: 22nd Symp. (Int.) Comb., 1063 (1988).
 (16) C. Chevalier, J. Warnatz: to be published in Prog. Energy Combust. Sci.
 (17) D.L. Baulch, T. Just, J.A. Kerr, M. Pilling, J. Troe, R.W. Walker, J. Warnatz: to be published in J. Phys. Chem. Ref. Data.
 (18) J. Troe, private communication.
 (19) N. Fujii, T. Asaba: J. Fac. of Eng. Univ. Tokyo (B) XXXIV, #1, 189 (1977).
 (20) M. Braun-Unkhoff, P. Frank, Th. Just: 22nd Symp. (Int.) Comb, 1053 (1988).
 (21) Y.Z. He, W.G. Mallard, W. Tsang: J. Phys. Chem. 92, 2196 (1988).
 (22) C.Y. Lin, M.C. Lin: J. Phys. Chem. 90, 425 (1985).
 (23) G.J. Gibbs, H.F. Calcote: J. Chem. and Eng. Data 4, 226 (1959).
 (24) E.S. Goloniva, G.G. Fyodorov: 6th Symp. (Int.) Comb., 88 (1956).
 (25) J. Warnatz: 18th Symp. (Int.) Comb., 369 (1981).
 (26) U. Maas, J. Warnatz: Comb. & Flame 74, 53 (1988).
 (27) A. Burcat, C. Snyder, T. Brabbs: NASA Technical Memorandum 87312 (1986).

Table 1
 Benzene mechanism and rate constants in cm³, mol, s, K, and kJ.

Reaction	A	B	Ea	Ref.
414. C ₅ H ₅ → 1- C ₅ H ₅	1.000e+14	0.0	188.0	20
415. 1- C ₅ H ₅ → C ₃ H ₃ + C ₂ H ₂	1.000e+14	0.0	71.1	20
449. C ₆ H ₅ → 1- C ₆ H ₅	4.000e+13	0.0	305.0	17
450. 1- C ₆ H ₅ → C ₄ H ₃ + C ₂ H ₂	2.000e+62	-14.7	241.0	20
451. 1- C ₆ H ₅ ↔ 1- C ₆ H ₄ + H	2.500e+58	-13.8	208.0	20
453. C ₆ H ₅ + O ₂ → C ₄ H ₄ + H + 2CO	1.000e+12	0.0	8.4	19
455. C ₆ H ₅ O → C ₅ H ₅ + CO	2.500e+11	0.0	184.0	17
456. C ₆ H ₄ OH → C ₅ H ₅ + CO	2.500e+11	0.0	184.0	17
457. C ₆ H ₆ ↔ C ₆ H ₅ + H	4.410e+29	-3.9	489.9	18
459. C ₆ H ₆ ↔ C ₄ H ₄ + C ₂ H ₂	1.000e+15	0.0	450.0	17
461. C ₆ H ₆ + H ↔ C ₆ H ₅ + H ₂	7.900e+13	0.0	41.8	19
463. C ₆ H ₆ + OH ↔ C ₆ H ₅ + H ₂ O	1.630e+08	1.4	6.1	17
465. C ₆ H ₆ + OH → C ₆ H ₅ OH + H	1.320e+13	0.0	46.0	17
466. C ₆ H ₆ + O ↔ C ₆ H ₅ + OH	3.612e+01	3.7	4.5	17
468. C ₆ H ₆ + O ↔ C ₆ H ₅ OH	3.612e+01	3.7	4.5	17
470. C ₆ H ₅ OH + H ↔ C ₆ H ₅ O + H ₂	1.144e+14	0.0	51.9	17
472. C ₆ H ₅ OH + H → C ₆ H ₆ + OH	2.230e+13	0.0	33.2	17
473. C ₆ H ₅ OH + OH ↔ C ₆ H ₅ O + H ₂ O	3.000e+12	0.0	0.0	17
475. C ₆ H ₅ OH + OH ↔ C ₆ H ₄ OH + H ₂ O	3.000e+12	0.0	0.0	17

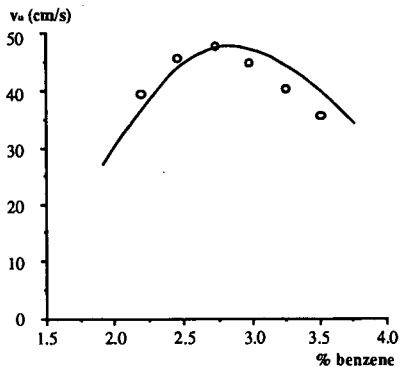


Fig. 1. Free flame velocities in benzene-air mixtures, $P = 1$ bar, $T_u = 298$ K. Points: measurements (23). Line: Calculation.

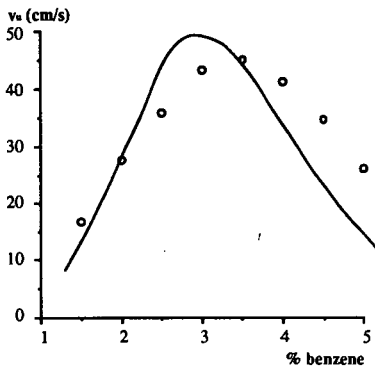


Fig. 2. Free flame velocities of benzene-20.8% oxygen-argon mixtures, $P = 1$ bar, $T_u = 298$ K. Points: measurements (24). Line: Calculation.

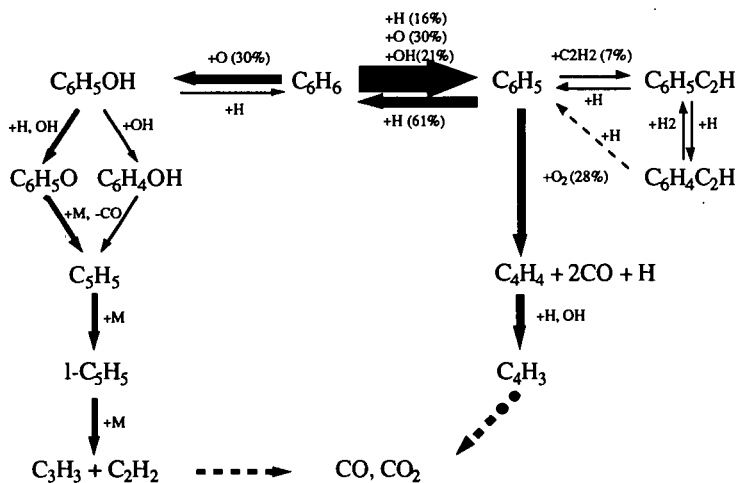


Fig. 3. Flow diagram for the oxidation of benzene in a stoichiometric flame, $P = 1$ bar, $T_u = 298$ K. The thickness of the arrows is proportional to the reaction rate integrated over the whole flame front

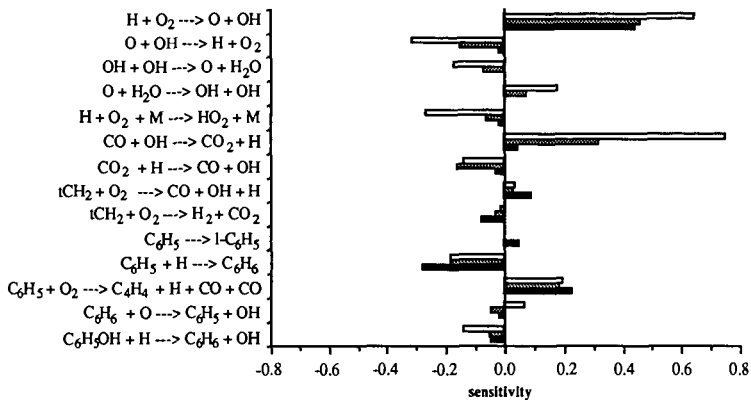


Fig. 4. Sensitivity analysis with respect to the laminar flame velocities in lean (white bars), stoichiometric (grey bars), and rich (black bars) benzene-air mixtures, $P = 1$ bar, $T_u = 298$ K.

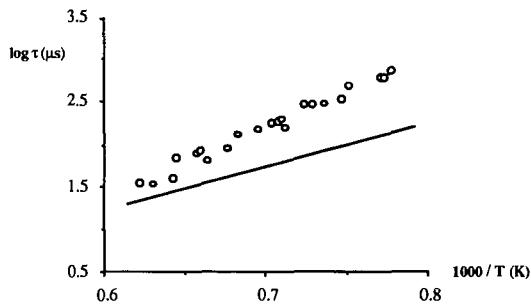


Fig. 5. Ignition delay times for stoichiometric benzene-oxygen-argon mixtures, $P = 2$ to 3 bar. Points: experimental values (27). Line: calculation.

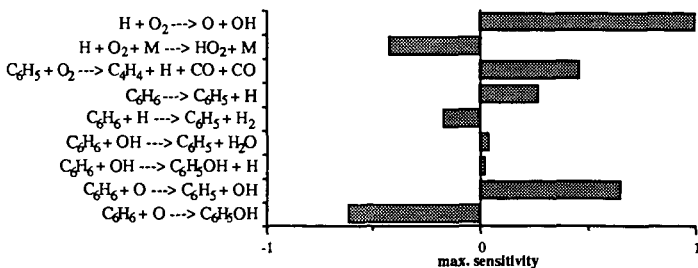


Fig. 6. Sensitivity test with respect to $[OH]$ concentration of a stoichiometric 1.69% benzene-12.675% O_2 mixtures diluted with argon, at $P = 2$ bar, $T_u = 1286$ K, and at $t = 30 \mu s$ ($\tau / 5$).

Preprint Submitted to the American Chemical Society
Fuels Division, National Meeting, New York City Aug. 1991

CYCLOPENTADIENE AND CYCLOPENTADIENYL CONVERSION DURING
BENZENE OXIDATION, THERMODYNAMIC AND MECHANISTIC CONSIDERATIONS.

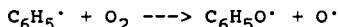
Joseph W Bozzelli, Viral Desai, Edward R Ritter and Anthony M. Dean* Dept of Chemical Engineering and Chemistry,
New Jersey Inst. of Technology, Newark, NJ 07039,
*Exxon Research And Engineering, Annandale, NJ 08801

Abstract

There are a number of studies on benzene oxidation and pyrolysis, yet we do not know of a detailed reaction mechanism based on fundamental kinetic and thermodynamic principles that explains published experimental observations. Benzene reacts by H transfer (abstraction) forming phenyl radicals. Prior to unimolecular decomposition, phenyl can react with O₂, O or HO₂ to form a phenoxy radical. Phenoxy, the major channel for benzene loss, has been shown to decompose to CO plus cyclopentadienyl radical. In this study, we focus on the oxidation pathways to loss of cyclopentadienyl species. We specifically consider thermodynamic and kinetic analyses for reactions of cyclopentadiene and cyclopentadienyl radical with O₂, O, H, OH and HO₂. Rate constants as functions of pressure and temperature for the radical addition and recombination reactions are calculated using bimolecular QRRK theory. We compare predictions from our mechanism with phenoxy and benzene reaction data.

INTRODUCTION

Benzene reacts in the presence of oxygen (through phenyl or cyclohexadienyl radical intermediates) to form phenyl and phenoxy radicals in addition to stable phenol molecules. Phenyl radicals in the presence of oxygen will undergo the rapid, exothermic, chain branching reaction:



The phenoxy and cyclohexadienyl radical intermediates are resonantly stabilized and are usually present at higher concentrations than the more reactive phenyl or other non-stabilized radicals. The phenoxy radical has been shown to unimolecularly react to produce carbon monoxide and cyclopentadienyl (CyCpdj) radical^{1,2}, while cyclohexadienyl radical produces methyl and CyCpdj³. Cyclopentadienyl radical is highly resonantly stabilized with references on its heat of formation ranging in value from 57 to 45 Kcal/mole corresponding to a resonance stabilization energy (RSE)^{4,5} of ca. 18 to 30 Kcal/mole. This large RSE essentially eliminates reaction of this radical with O₂ to form a peroxy radical, which is favorable for normal alkyl radicals. This occurs due to the very low, ca 11 Kcal/mole, well depth for

stabilizing the adduct with significant loss of entropy.

Our initial attempts to construct a mechanism comprised of elementary reactions to model benzene production and loss, for comparisons to our experiments on chlorobenzene and dichlorobenzene pyrolysis reaction in H_2 ,^{3,6} chlorobenzene oxidation⁶ or the benzene oxidation data of Brezinsky⁷, have produced relatively large concentrations of cyclopentadienyl radical (Cycpdj). Calculations, incorporating abstraction reactions for this radical, indicate it would build up to concentrations equal to or larger than its cyclopentadiene parent and would clearly act as a bottle-neck to benzene loss. The reactions in our mechanisms included microscopic-reversibility and showed that the benzene, phenyl, cyclohexadienyl - phenoxy system would essentially remain at steady state.

Phenols and phenoxy species are known to be common intermediates in oxidation of aromatic species and they are considered strong candidates as precursors in formation of dibenzofurans and dioxins. Knowledge of important reactions of phenoxy decomposition products - Cycpdj and its parent is therefore critical to understanding possible formation of dibenzofurans and dioxins, through reverse reactions, as well as their destruction.

Aromatic species are also important in motor fuels, with small ring aromatics often used to increase octane rating in gasolines⁷ since lead has been eliminated as a blending ingredient. Understanding the fundamental reactions of these aromatic species will clearly benefit researchers who are working to understand preignition and engine knock. This understanding may also have implications for soot formation in diesels.

In formulating a detailed model of benzene destruction and/or formation in varied oxidation or pyrolysis environments, we need to consider the decomposition pathways for these resonantly stabilized cyclopentadienyl and phenoxy species. We currently do not know of any reaction mechanism for benzene oxidation comprised of elementary reactions, which are based upon fundamental thermochemical kinetic principles. Brezinsky⁷ and Venkat et. al.⁸ have published general reaction schemes, with no rate constants or thermodynamic properties. Bittker³ published a mechanism which was based upon previously published reaction paths and presented rate constants which fit experimental data for ignition delay times and toluene loss profiles. Bittker, however, used a sensitivity code to determine the important reactions and then optimized the fit of the data by adjusting rate constants. No account for collisional fall-off of activated complexes formed by addition of atoms or radicals to unsaturated (olefinic or aromatic) bonds, or by combination of radical species was included. Published mechanisms for toluene and other aromatic pyrolysis sometimes include reactions where the Arrhenius A Factor is reasonably close to the high pressure limit value, but the activation energy is significantly less than the known bond energy or energy barrier at the appropriate temperature. This serves to dramatically accelerate the reaction, instead of

slowing it down, as would occur if it were in the fall off region, and when E_a is less than ΔH_{rxn} , it also appears to violate with thermodynamics. The exception, where one would expect to have a lower E_a is only if one were well away from the high-pressure limit, implying a much lower Arrhenius A factor. The unrealistic combination of a high A and low E_a serves to dramatically, but erroneously, accelerate the reaction.

In this study we focus on thermodynamic and kinetic analysis for reaction paths of cyclopentadiene and cyclopentadienyl radical with O_2 , O and H atoms, in addition to OH and HO_2 radical. These reaction paths are radical combination or addition to unsaturated bonds in the cyclopentadienyl ring which form energized complexes that can react back to reactants or to low energy products before being collisionally stabilized. We treat all of these reactions with the bimolecular Quantum Rice Ramsperger Kassel Theory (QRRK)¹¹. We also treat dissociation of the complexes which become stabilized with unimolecular QRRK theory to account for collisional fall-off at temperatures of the experimental data we are modeling. Required thermodynamic properties for the radical intermediates were calculated using the THERM¹² computer code.

Metathesis reactions of cyclopentadiene with H, OH, HO_2 , phenyl, phenoxy, and alkyl radicals all serve to abstract the weak allylic hydrogen and form the resonantly stabilized radical. These reactions are relatively fast at combustion temperatures and serve to form and maintain a relatively high concentration of Cycpdj, which remains in thermal equilibrium with the rest of the radical pool. Clearly when the Cycpdj builds up in concentration the reverse reactions become important. The abstraction reactions, therefore, serve to shuttle the H atoms back and forth between resonantly stabilized and other species with relative concentrations controlled more by thermodynamics (equilibrium) than by kinetics. We propose that radical addition and combination reactions involving these resonantly stabilized species play a major role in the oxidation loss processes of benzene.

Addition Reactions of H, OH, and O atoms to Cyclopentadiene

The addition of a radical such as OH or H to the parent Cycpd forms an energized adduct, which can decompose to lower energy, non-cyclic products by Beta Scission (B_{sc}) reactions, dissociate back to reactants or be collisionally stabilized. There are two sites that a radical can add to the Cycpd molecule, the 1 or the 2 position, where the 5 position is carbon with 2 hydrogens. If a radical or atom adds to the 1 position, a radical is formed at the 2 position, which can B_{sc} the allylic carbon-carbon bond, opening the 5 member ring and forming a stabilized radical. If an atom or radical adds to the 2 position a radical is formed at the 1 position, which B_{sc} a vinylic carbon-carbon bond opening the ring and forming a vinylic radical. The formation of a vinylic radical is less thermodynamically favored, but the vinylic radical, if formed, will rapidly decompose, unimolecularly, by a series of scission reactions to acetylene plus a

radical.

The example of H atom adding to the double bond of Cycpd at the 1 position is shown in Figure 1. Here the cyclic radical can decompose to a lower energy linear C_5 dienyl radical, which also has a large amount of resonance stabilization and is therefore not highly reactive. The addition of H atoms to the 2 position in the ring results in a non-resonantly stabilized cyclic radical, which can either dissociate back to reactants or undergo ring opening to form a 1,4-pentadiene-1-radical (vinyllic) that will rapidly dissociate to acetylene and the relatively stable allyl radical. Thus the more energetic pathway, although slower, serves, essentially, as an irreversible sink and is important.

The addition of OH to Cyclopentadiene (Fig 2) at the 2 position forms a radical at the 3 position (carbon adjacent to the CH_2 group). This radical will either dissociate back to initial reactants or B_{sc} a carbon-carbon bond to form a vinyllic alcohol labeled C^*CCOHC^*C . (* denotes a double bond). This will either react back to the cyclic radical, beta scission to an endothermic channel forming acetylene and a resonantly stabilized primary alcohol radical of propenol as labeled in channel 3. An alternate reaction path of the linear C_5 vinyl radical, however, is a hydrogen shift from the alcohol to the vinyl group with the oxy radical then initiating the scission reaction to either vinyl + propene aldehyde or $C^*C(C^*O)C^*C + H$. These carbonyl products will eventually react to $CO +$ unsaturated C_2 and CH_3 hydrocarbons. OH adding to the 1 position will allow B_{sc} of an allylic C-C bond to form $C.C^*CC^*COH$ which is equivalent to $C^*CC^*CC.OH$, and will beta scission to $C^*CC^*CC^*O + H$. This linear unsaturated C_5H_6O will lose the carbonyl H atom (abstraction) and break down to acetylenes plus CO. Reactions of O atoms with CycPD are also very important.

Reactions of Cyclopentadienyl Radical (CycPd_j)

CycPd_j + HO₂
In the benzene oxidation mechanism we have assembled, the reaction of CycPd_j + HO₂ is one of the most important chain branching reactions. These two radicals build up to relatively high concentrations at temperatures of the experiments we are modeling (ca 1000 - 1200 K), and this reaction is, therefore, important to reducing both radical concentrations. The potential energy level diagram illustrated in Figure 3 shows that combination of the two radicals can form a hot cyclopentadienyl hydroperoxide which will rapidly dissociate either back to reactants or to cyclopentadienyl-oxy (Cpd-oxy) radical + OH, with the products favored at these temperatures due to slightly lower exit barrier and the increased entropy. The OH product is also more reactive than HO₂, further accelerating the overall reaction via abstraction reactions.

The Cpd-oxy radical will undergo rapid unimolecular dissociation at these temperatures via two low energy pathways shown in Figure 4. One path forms a cyclopentadienyl ketone + H atom, and the second opens the ring to a vinyllic pentadienyl aldehyde

radical. This will undergo rapid internal abstraction of the carbonylic hydrogen to form the resonantly stabilized complex shown in figure 4. The carbonyl radical formed will dissociate to CO plus a butadienyl radical which will further dissociate to acetylene + vinyl.

We note that the above Cpd-oxy radical (adduct) is also formed directly from the combination of O atoms with CyCpdj, but in this case, the adduct formed (initially) has 50 kcal/mole more energy than is needed to undergo B_{SC} reactions to the products in Fig. 4. This reaction is only limited by [O].

Several of the above reaction paths including O atom addition to either CyCpd or CyCpdj result in formation of cyclopentadien-1-one. This ketone can further react through addition of radical species to its unsaturated bonds, as shown in Fig. 5 for H atom addition. The initial adduct has enough energy to undergo ring opening forming a stabilized carbonyl radical, which will further decompose by unimolecular reaction to CO + butadienyl radical.

We have treated these reaction systems with the bimolecular QRRK formalism of Dean¹¹ to determine the apparent reaction rate constants to each channel including the stabilized adducts. Input parameters for the QRRK calculation are listed in below for reaction illustrated in Fig 5.

k	A	E_a (Kcal/mole)	Reference
k_1	3.98E13	2.6	A and E_a from $H + C_2H_4$, ref (11)
k_{-1}	1.53E14	47.74	Thermodynamics
k_2	7.83E14	18.22	Thermodynamics
k_{-2}	6.77E12	10.0	A TST, $\Delta S^\ddagger = -4$, E_a (Ring Strain + 5 ¹³)
k_3	1.47E15	38.44	($\Delta H_{Rxn} + 5^{13}$)

(* denotes double bond, # denotes triple bond)

References

1. M. C. Lin and C. Y. Lin, J. Phys. Chem. 90, 425 (1986).
2. J. Manion and R. Louw, J. Phys. Chem., 93, 3563 (1989).
3. E. Ritter, J. Bozzelli and A. M. Dean, J. Phys. Chem 94, 2493. (1990), E. Ritter Ph.D Thesis NJIT (1989).
4. D. McMillen and D. Golden, Ann. Rev. Phys. Chem. 33, 493 (1982)
5. S. Stein and D. M. Golden, J Org. Chem, 42, p839 (1977)
6. E. Ritter and J. W. Bozzelli, Chemical Phys Processes in Combustion Combustion Inet., Eastern States Section Albany, NY (1989).
7. K. Brezinsky Prog in Energy Combust Science, 12, (1986).
8. C. Venkat, K. Brezinsky and I. Glassman, 19 Symp. Combustion, 143 (1982)
9. D. A. Bittker Central States Section, Combustion Institute Symposium, Indianapolis, In, May 1988.
10. L. D. Brouwer, W. M. Margraf and J. Troe, J Phys. Chem. 92, 4905 (1988).
11. A. M. Dean, J. Phys. Chem. 89, 4600, (1985).
12. THERM Thermodynamic Property Estimation of Radicals and Molecules, E. Ritter and J. W. Bozzelli, Int. J. Chem Kinetics (1991).
13. S. Stein and A Fahr, Proceedings of 22nd Comb. Inst. Symp, 1023 (1988).

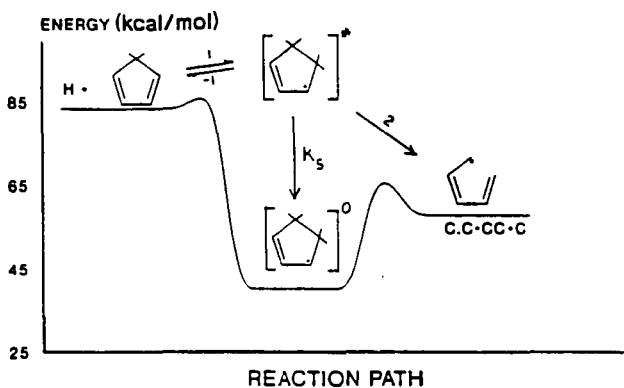


FIGURE 1. CYCLOPENTADIENE + H \rightarrow PRODUCTS

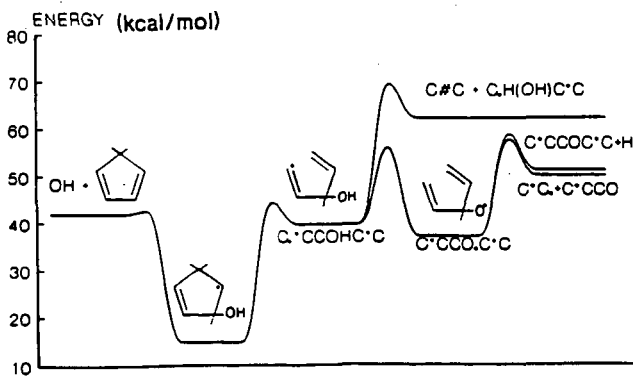


FIGURE 2. CYCLOPENTADIENE + OH \rightarrow PRODUCTS

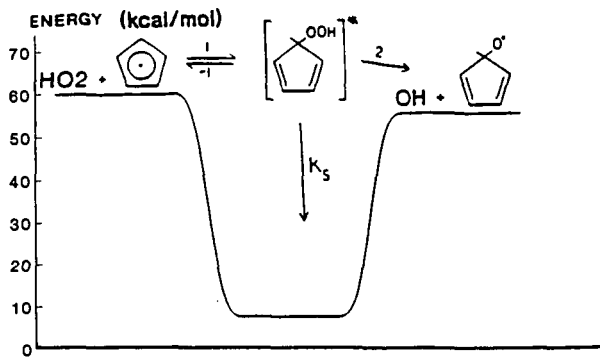


FIGURE 3. HO₂ + CYCLOPENTADIENYL RADICAL

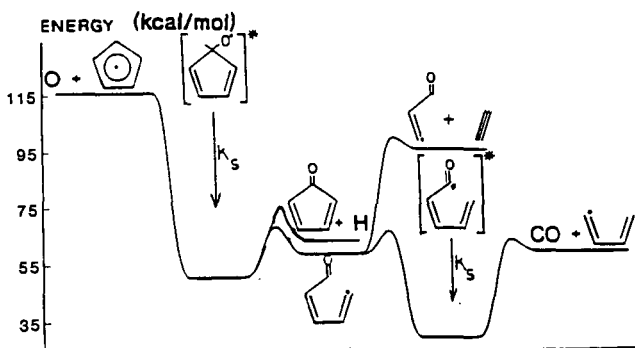


FIGURE 4. O + CYCLOPENTADIENYL RADICAL

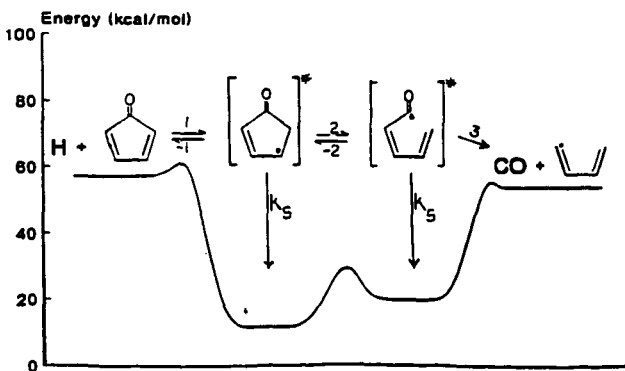


FIGURE 5. H + CYCLOPENTADIEN-ONE